Articles

Computer Models of DNA Four-Way Junctions†

A. R. Srinivasan and Wilma K. Olson*

Department of Chemistry, Wright-Rieman Laboratories, Rutgers, the State University of New Jersey, New Brunswick, New Jersey 08903

Received October 26, 1993; Revised Manuscript Received May 10, 1994®

ABSTRACT: A modeling scheme that combines a constrained backbone generating algorithm with simple hard-sphere packing calculations is offered to build the four-stranded structures of DNA found in Holliday junctions. Two standard B-DNA duplexes are oriented side by side with helix axes at different relative inclinations and then systematically rotated and translated to identify closely spaced contact-free states. Attempts are subsequently made to introduce a low-energy sugar–phosphate linkage that serves as the site of strand exchange between the two duplexes. The chemical connection is sought using an algorithm which identifies the possible arrangements of the intervening backbone torsions between arbitrarily positioned bases. The goal is to identify the multiple conformational solutions associated with a particular arrangement of neighboring DNA helices in the four-way junction rather than a single optimum structure. The methodology is general, in terms of accommodating four-way junctions with arms of variable conformation and chain length and of dimensions much greater than treated heretofore. The only deformation in the four-way structures relative to B-DNA occurs at the site of backbone exchange, with base stacking and Watson–Crick pairing completely preserved in all models. The arrangements of neighboring bases at these sites resemble the unusual conformational steps found in a number of small molecule nucleic acid crystal structures. An interesting outcome of the calculations is the formation of sterically acceptable four-arm Holliday junctions over a wide range of angles at the cross. The potential mobility of the Holliday junctions is inferred from visualization and energetic analysis of the various models. Long-range electrostatic energies based on different currently available treatments of the dielectric constant are used to estimate the conformational preferences and flexibility of the four-stranded structures. The various dielectric schemes, however, are not in complete agreement on the likely conformational variability of the four-way junctions. The structures suggest a possible mechanism for branch migration and detail a pathway linking the antiparallel uncrossed Holliday structure inferred from solution measurements and the parallel cross-packed helical arrangements observed in single-crystal X-ray studies.

Cellular processes can impose major structural deformations of the DNA double helix. The strand exchange resulting from genetic recombination, for example, proceeds via a four-stranded branched interwound form termed a Holliday junction (Holliday, 1964). This unusual structure, represented schematically in Figure 1, arises when two homologous DNA duplexes become nicked and exchange single strands upon rejoining. The junctions produced in naturally occurring linear chains, however, are unstable because of a 2-fold symmetry in sequence and dissociate spontaneously into duplexes through migration of the branch along one of the arms of the four-stranded DNA (Thompson *et al.*, 1976; Robinson & Seeman, 1987). When produced in closed circular DNA, the four-way junctions generate characteristic figure-eight trajectories that can be visualized under the electron microscope (Potter & Dressler, 1976, 1978; Hoess *et al.*, 1987; Kitts & Nash, 1987; Nunes-Düby *et al.*, 1987), confirming the presence of the structural intermediate.

Clever synthetic design that breaks strand symmetry but ensures the occurrence of stable base pairs (Seeman, 1982; Seeman & Kallenbach, 1983) has succeeded in immobilizing model four-stranded junctions, permitting a wide range of solution studies. The conformational picture that has emerged is one of a semirigid base-stacked structure consistent with the overall geometry of an "X" (Cooper & Hagerman, 1987, 1989; Churchill *et al.*, 1988; Duckett *et al.*, 1988; Murchie *et al.*, 1989; Lilley & Clegg, 1993a,b; Clegg *et al.*, 1994). In solutions containing Mg^{2+}, two pairs of interconnected duplexes appear to associate such that one strand of each retains the approximate B-type conformation it would have in an ordinary double helix, while the complementary strands form sharp U-turns at the site where the exchange of partners occurs (Cooper & Hagerman, 1987; Duckett *et al.*, 1988). In addition, the base pairs flanking the branch site remain paired at low temperatures in the presence of divalent counterions (Seeman *et al.*, 1985; Wemmer *et al.*, 1985). This antiparallel form, however, is only slightly more stable than a parallel model in which the strands cross one another at the junction point (Lu *et al.*, 1991; Fu & Seeman, 1993). In the absence of any metal ions, the four-arm structure adopts a maximally extended form with base pairs at the branch point partially or fully associated at low temperatures (Wemmer *et al.*, 1985; Duckett *et al.*, 1988, 1990; Chen *et al.*, 1991).

Additional support for the X-structure comes from the observed crossed packing of DNA duplexes in several recent crystal structures (Timsit *et al.*, 1989, 1991; Heinemann *et al.*, 1992; Baikalov *et al.*, 1993; Lipanov *et al.*, 1993). It is possible to construct stereochemically reasonable models of

† Sponsorship of this research by the U.S. Public Health Service under Research Grant GM20861 is gratefully acknowledged.

® Abstract published in *Advance ACS Abstracts,* July 15, 1994.

0006-2960/94/0433-9389$04.50/0

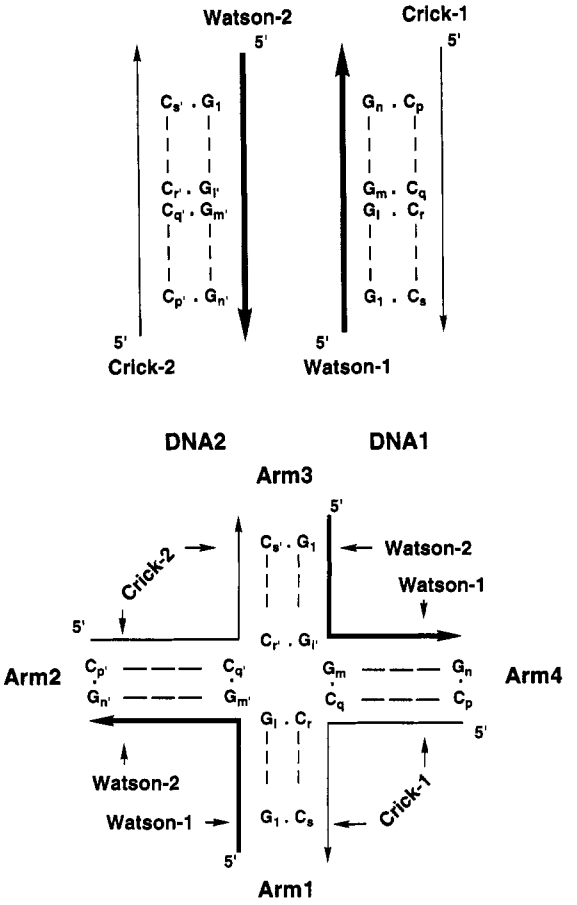

FIGURE 1: Schematic representation of homologous DNA duplexes (a, top) prior to formation of the four-way Holliday junction and (b, bottom) following exchange of strands between G_l on DNA1 and $G_{m'}$ on DNA2 and between $G_{l'}$ on DNA2 and G_m on DNA1.

Holliday junctions on the basis of the coordinates of the B-type d(ACCGGCGCCACA)·d(TGGCCGCGGTGT) duplex (Timsit & Moras, 1991). Except for the mutual orientation of helical axes, these models are strikingly similar in overall appearance to early hand-built representations of the crossed strand exchange between homologous DNAs (Sigel & Alberts, 1972). The original parallel models with helical axes pointing in the same direction and with zero vertical translation have been criticized on the basis of both the small entropic factor (*i.e.*, limited flexibility) presumably associated with such arrangements and the highly unfavorable electrostatic interactions between the closely spaced arms of the DNA (von Kitzing *et al.*, 1990). The close contacts between DNA helices in the crystal are only possible because of the presence of cations in the vicinity of the charged phosphate groups. Indeed, the best diffracting crystals are obtained with a stoichiometric excess of Mg^{2+} ions per nucleotide chain unit (Timsit & Moras, 1991). Detailed atomic models consistent with the overall solution properties of the four-way junctions can also be constructed using standard molecular mechanics packages. Energetically optimized structures are readily obtained given a reasonable initial model. The final structure, however, is not dramatically altered in overall conformation from the assumed starting structure. Both antiparallel X and "square-planar" arrangements of Holliday structures have been constructed in this manner (von Kitzing *et al.*, 1990).

The apparent spatial similarity of the four-stranded X to the predicted contacts of double helices in long interwound DNA supercoils (Hao & Olson, 1989; Zhang *et al.*, 1991; Yang *et al.*, 1993) introduces a new structural basis for the well-appreciated role of supercoiling in genetic recombination (Wasserman & Cozzarelli, 1986). The potentially wide ranging flexibility of the supercoil (Schlick & Olson, 1992; Schlick *et al.*, 1994) as well as the above cited ease of interconversion of Holliday junctions between parallel, antiparallel, and open forms points to the need for a continuum of four-stranded models. The fluorescence energy transfer experiments used to determine the mean separation between ends of model four-arm DNA junctions (Murchie *et al.*, 1989; Eis & Millar, 1993) might also benefit from a more dynamic structural interpretation. A treatment of overall structural mobility could additionally provide new molecular insight into the conformational processes involved in branch migration.

In this report, as a first step toward achieving a more dynamic picture of branched DNAs, we outline a general procedure to build arbitrary four-way junctions. We take advantage of a constrained model building scheme previously developed to study the conformations of ordinary and unusual DNA double helices (Srinivasan & Olson, 1986, 1987; Jin *et al.*, 1993) along with recent hard-sphere calculations introduced to assess the closest packing of DNA double helices (Srinivasan & Olson, 1992). We start by generating feasible models of the B-type double helix and then orient pairs of duplexes in stereochemically acceptable spatial arrangements. We consider various mutual orientations and rotations of the helical axes and search for local backbone geometries that link closely positioned base pairs at the site of potential recombination. We assume that base pairs retain the stacking found in the original helices with the only conformational changes occurring at the nucleotide sites of the chemically rearranged sugar–phosphate backbone. We rank the resulting solutions on the basis of various energy estimates and conformational counting schemes. The methodology is quite general, being able to accommodate four-way junctions with arms of variable conformation and chain length and of sizes much greater than treated heretofore. The reported models are useful starting points for more elaborate computer simulations of DNA four-way junctions.

MATERIALS AND METHODS

Overview. Two DNA molecules, designated DNA1 and DNA2 in Figure 1a, are used to build the Holliday intermediates formed upon recombining model $dG_n \cdot dC_n$ and $dG_{n'} \cdot dC_{n'}$ oligonucleotide duplexes in various spatial dispositions. The chain crossover takes place at the centers of contacted strands of identical sequence but of opposite polarity. Specifically, the G-strand of DNA1, termed Watson-1 in the figure, and the G-strand of DNA2, termed Watson-2, become nicked and recombine with one another rather than reclose to the starting duplexes. The C-strands of DNA1 and DNA2 (Crick-1 and Crick-2, respectively) remain intact in this scheme, running in an antiparallel chemical sense. The site of backbone cutting occurs between bases G_l and G_m in DNA1 and $G_{l'}$ and $G_{m'}$ in DNA2. Upon chain closure, phosphate linkages join G_l of DNA1 with $G_{m'}$ of DNA2 and $G_{l'}$ of DNA2 with G_m of DNA1. The resulting junction, with 5′–3′ strand polarity maintained in all four single strands, is represented as a cross in Figure 1b. Alternatively, if DNA2 is moved in the plane of the paper (Figure 1a) to the right side of DNA1, the strand crossover will entail contacted C-strands. In this case, the backbones between $C_{q'}$ and $C_{r'}$ of DNA2 and C_q and C_r of DNA1 will open, and the new chemical linkages will connect C_q with $C_{r'}$ and $C_{q'}$ with C_r. Exploratory computations with C–C crossovers indicate results that are similar to the G–G exchanges. Only the exchange of G-containing strands is thus reported in this study.

The current calculations are designed to generate four-way junctions with arms of arbitrary chain length and conformation. The different fragments can be useful for introducing base sequence-dependent structural features in the DNA and for understanding four-way junctions in the context of DNA supercoiling. Starting duplexes with $n = 20$ base pairs (bp) are employed here so that the arms of the resulting four-way junctions correspond to approximately one full turn of B-DNA.

Starting Duplexes. Eight different DNA structures (described in Table A1, supplementary material) are used as starting models for DNA1 and DNA2. These idealized structures, generated with the constrained model building procedure outlined below, are similar in overall morphology to the canonical B-DNA helix (Chandrasekaran & Arnott, 1989). Adjacent base pairs are perfectly parallel in the starting duplexes with local roll and tilt angles of 0° and twist angles of 36° compared to corresponding values of 0°, 0.8°, and 35.8° in the ideal B-DNA fiber model [see Olson *et al.* (1988) and Nauss (1992) for mathematical definitions of parameters]. The x,y,z coordinates of these DNA structures are initially expressed, as detailed elsewhere (Srinivasan & Olson, 1992), in an orthogonal coordinate frame with the reference x–y plane coinciding with the starting base-pair plane. The z-axis thus runs parallel to the helix axis of an ideal B-DNA double helix. The origin of the reference frame lies in a plane midway between the two central base pairs of the initial intact duplex. The x-axis is chosen to run parallel to the C8–C6 vector of one of the base pairs, and the y-axis, which is aligned along the pseudodyad of the starting base pair, is chosen to form a right-handed coordinate system. This definition of coordinate frame allows a general treatment of the Holliday junction without placing restrictions on either the sequence or length of the associated DNAs. The acyclic backbone torsions $-\phi'$, ω', ω, ϕ, ψ–, the phase angles of pseudorotation P, and the glycosyl torsions χ of the different starting states are compared in the Appendix (supplementary material) with the corresponding parameters in the canonical B-DNA duplex. The major and minor groove widths and the estimated per residue nonbonded interaction energy are also tabulated, and the procedures employed to determine the former values are described in detail. It is clear from the data that, except for model 5 with altered (ψ and ϕ') torsions about the C5′–C4′ and C3′–O3′ bonds, the backbones of all of the starting helices are very similar to the standard B-DNA double helix. Model 5 is also a slightly higher energy structure (by ~2–3 kcal mol^{-1} per residue) than the other starting duplexes.

Spatial Disposition. The relative displacement and orientation of DNA1 and DNA2 are described in terms of the six interhelical parameters (θ, $\theta 1$, $\theta 2$, Δx, Δy, Δz) illustrated in Figure 2. The two DNAs are initially superimposed in one of the eight double-helical forms listed in the Appendix. The atoms of DNA2 are then rotated by $180° - \theta$ about the x-axis (as defined above) and translated by Δx, Δy, and Δz along the x-, y-, and z-axes, respectively. The new coordinate $\mathbf{x}_i'$ of atom i in DNA2 is related to the original coordinate $\mathbf{x}_i$ of atom i in the starting reference frame (*i.e.*, DNA1) by the transformation:

$$\mathbf{x}_i' = \begin{bmatrix} 1 & 0 & 0 \\ 0 & \cos\theta & -\sin\theta \\ 0 & \sin\theta & \cos\theta \end{bmatrix} \mathbf{x}_i + \begin{bmatrix} \Delta x \\ \Delta y \\ \Delta z \end{bmatrix} \quad (1)$$

The rotation θ positions DNA2 with respect to DNA1 in an arbitrary azimuthal orientation, the parameter being varied from 0° to 180° at increments of ±45°. The relative vertical slippage of the DNAs, Δz, and the slippage of helical centers,

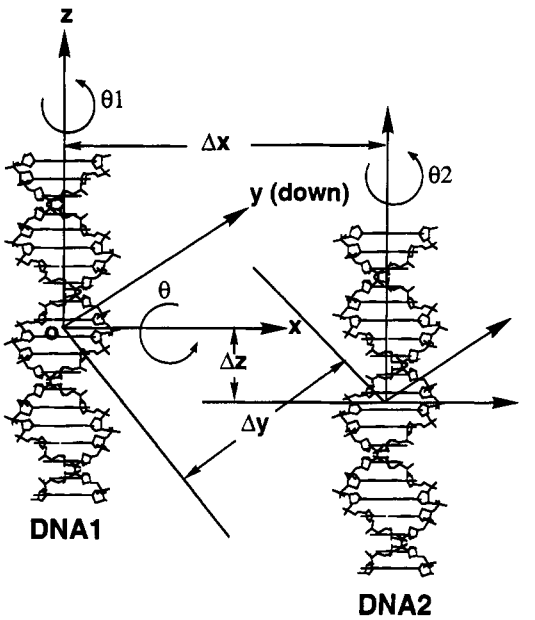

FIGURE 2: Translational (Δx, Δy, Δz) and rotational (θ, $\theta 1$, $\theta 2$) parameters used to describe the relative displacement and orientation of closely associated DNA duplexes (DNA1 and DNA2).

Δy, are altered at intervals of 1 Å from –5 to 5 Å, while the contact distance between helices, Δx, is varied at intervals of 1 Å over the range –22 to –16 Å. The $\theta 1$ and $\theta 2$ parameters in Figure 2 are rotations associated with the slithering (Benjamin & Cozzarelli, 1986) of the helical axes with respect to one another. These rotations bring different parts of the helical surfaces into direct contact. For each (Δx, Δy, Δz, θ) combination, the $\theta 1$ and $\theta 2$ screw rotations are varied from –60° to 60° at 10-deg intervals. The chosen limits for the horizontal translations, the vertical slippages, and helical axis rotations ($\theta 1$ and $\theta 2$) are based on previous knowledge of the short-contact free packing arrangements of B-DNA double helices in different azimuthal orientations (Srinivasan & Olson, 1992). Initial trials were made using reasonably large translational and rotational intervals (2 Å and 20°, respectively) in order to limit computational time. Fairly extended ranges for the parameters have been incorporated in the final calculations so as to include as many four-way junctions as possible.

Single-Strand Crossover. Once the duplexes are positioned, attention is focused on the four sugar–base fragments of DNA1 and DNA2 adjoining the proposed branch point of the four-way junction (residues G_l, G_m, $G_{l'}$, and $G_{m'}$ in Figures 1 and 3). The phosphate linkages connecting nucleosides l to m and l′ to m′ are removed to simulate nicks present in the two strands prior to recombination. The feasibility of chain crossover is then tested by attempting to place phosphate groups between nucleosides l and m′ and between l′ and m on different helical strands. This is achieved by application of a constrained model-building algorithm previously developed for the study of regular duplex structures (Srinivasan & Olson, 1987). The procedure generates a range of acceptable backbone conformations for each given arrangement of nucleic acid bases rather than simply an optimum structure. The glycosyl torsion between the sugar and base and the sugar geometry (both the ring puckering and the exocyclic C5′–C4′ torsion) are treated as independent variables. The separations of O3′ and O5′ atoms determined by these variables are used to gauge chain closure. When these distances conform to the known geometry of phosphate chemical bonding, an intervening phosphorus atom with correct C–O–P valence angles and oxygen side groups

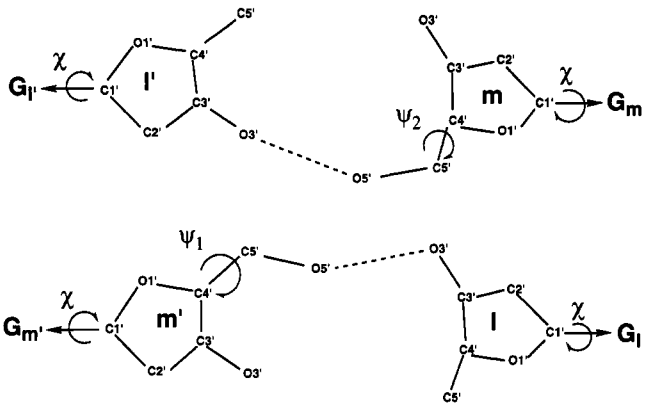

FIGURE 3: Nucleoside fragments and local conformational parameters of nicked DNA duplexes adjoining the branch point of a four-way junction. See Figure 2 for relative locations of residues l, m, l′, and m′ in associated DNA duplexes.

is introduced. The resulting structures are then analyzed on the basis of potential energy and conformational classification (see below).

The choice of starting duplex fixes the glycosyl and sugar torsions of the four-way junction (see Appendix). These predetermined values establish the positions of the O3′ atoms in nucleosides l′ and l of the nicked helical model. The only independent local conformational variables are thus the exocyclic C5′–C4′ torsions (ψ_1 and ψ_2 in Figure 3), which are allowed to vary at 10-deg increments over the entire 360° angular range. The choice of ψ acting in concert with the sugar–base geometry characterizing a particular helix determines the locations of the O5′ atoms in residues m′ and m. In order to form the junctions, the O3′ and O5′ atoms of nucleosides on different duplexes must be successfully connected (noted by the dashed line in Figure 3). As outlined below, it is necessary to carry out two such interstrand searches in order to construct a four-way junction involving residues l, m, l′, and m′. To rebuild the original duplexes, the O3′ and O5′ atoms in adjacent residues on the nicked strands can be rejoined.

Local Conformational Energy. Preliminary estimates of the energies of local junctions are made using potential functions and constants described elsewhere (Srinivasan *et al.*, 1987). The potential energy V is expressed as a sum of pairwise van der Waals repulsions, London attractions, Coulombic interactions, and charge-induced polarizability contributions between all nonbonded atom pairs (i and j) whose distance (r_{ij}) varies in the different four-way structures and is computed as a function of the inter- and intrastrand parameters of the local four-way junctions (*i.e.*, θ, $\theta 1$, $\theta 2$, Δx, Δy, Δz, P, χ, and ψ).

$$V = \sum_i \sum_j \frac{A_{ij}}{r_{ij}^{12}} - \frac{B_{ij}}{r_{ij}^{6}} + \frac{332\delta_i\delta_j}{\epsilon r_{ij}} - \frac{166(\delta_j^2\alpha_i + \delta_i^2\alpha_j)}{\epsilon r_{ij}^4} \quad (2)$$

The van der Waals constants A_{ij}, London constants B_{ij}, partial charges δ, and polarizabilities α in eq 2 are determined by the chemical nature of the interacting atoms. The composite energy is well-known to provide a reliable estimate of local nucleic acid conformational preferences (Olson & Srinivasan, 1990). The dielectric constant ϵ is assigned a value of 4 in the preliminary calculations involving local junctions but is treated as a distance-dependent variable in subsequent polymeric models (see below). The numerical factors in eq 2 are chosen to yield energies in kilocalories per mole when the distance is expressed in angstrom units and the charge as fractional electronic charge. The influence of the local ionic environment is treated indirectly through reduction of the net charge at the phosphate group by 0.78 esu (*i.e.*, $\delta_{phosphate}$ = −0.22 esu) (Srinivasan & Olson, 1980; Taylor & Olson, 1983), in accordance with the concepts of counterion condensation theory (Manning, 1978). This is accomplished in the all-atom models by modifying the residual charges on the pendant oxygen atoms of the phosphodiester. The level of charge reduction is based on the spacing of residues in standard B-DNA helices and the assumption of condensed monovalent counterions. (The theoretically estimated amount of charge condensation per phosphate unit would shift from 0.78 esu to 0.88 esu if the monovalent counterions considered in this study were replaced by divalent ones.) No specific contributions are included for the crossover site. While the degree of condensation is apt to differ at the crossover point of a four-stranded model, our approximation is unlikely to lead to qualitatively incorrect results. First, the B-DNA value is appropriate for the helical arms, which are critical in determining long-range conformational preference. Second, a potential with invariant effective charges is better than a potential with bare charges (valence = −1) (Fenley *et al.*, 1994). The per residue charge is concentrated on a single P atom in selected approximations of the long-range electrostatic energy.

Long-Range Electrostatic Energy. The dielectric constant used in the electrostatic calculations of the extended four-way helical junctions is chosen to mimic the long-range screening of electrostatic interactions by solvent. As a first approximation, ϵ is set equal to the dielectric constant of water (ϵ_∞ = 78). At the next level of approximation, two simple distance-dependent functions are employed. The most primitive is a simple linear suppression term where $\epsilon(r_{ij}) = r_{ij}$ (Miller, 1979; Kollman *et al.*, 1981) and the next a standard Debye–Hückel screening term, $\epsilon(r_{ij}) = \epsilon_\infty \exp(r_{ij}/D)$, where D is the Debye length (a constant proportional to the ionic strength, here taken to be 10 Å corresponding to a salt concentration of ~0.1 M). Four different sigmoidal dielectric functions are also considered. The first, developed by Hingerty *et al.* (1985), mimics the binding of selected cations with the GpC monoanion.

$$\epsilon(r_{ij}) = \epsilon_\infty - (\epsilon_\infty - 1)\left(\frac{r_{ij}}{2.5}\right)^2 \frac{\exp\left(\frac{r_{ij}}{2.5}\right)}{\left(\exp\left(\frac{r_{ij}}{2.5}\right) - 1\right)^2} \quad (3)$$

The second, due to Lavery and co-workers (Lavery, 1988; Ramstein & Lavery, 1988), accounts for the observed X-ray structure of oligomeric B-DNA and also reproduces the fixed fraction of counterions condensed on the surface of the double helix (Fenley *et al.*, 1990).

$$\epsilon(r_{ij}) = \epsilon_\infty\left(1 - \left(\frac{1}{2}\left(\frac{r_{ij}}{6.25}\right)^2 + \left(\frac{r_{ij}}{6.25}\right) + 1\right)\exp\left(\frac{-r_{ij}}{6.25}\right)\right) \quad (4)$$

The third, introduced by Mazur and Jernigan (1991), mimics the salt-dependent B to A transition in base-pair models of the poly(dG)·poly(dC) duplex.

$$\epsilon(r_{ij}) = \epsilon_\infty \left(\frac{\exp\left(\frac{1.8r_{ij}}{r_{mid}}\right)^p + \exp\left(-\left(\frac{1.8r_{ij}}{r_{mid}}\right)^p\right)}{\exp\left(\frac{1.8r_{ij}}{r_{mid}}\right)^p - \exp\left(-\left(\frac{1.8r_{ij}}{r_{mid}}\right)^p\right)} - \left(\frac{r_{mid}}{1.8r_{ij}}\right)^p \right) \quad (5)$$

The parameter r_{mid} in the last equation is related to the ionic strength of the surrounding environment and is equal to the distance at which $\epsilon = \epsilon_\infty/2$. Two forms of the equation are considered with the coefficient p set equal to 1 or 2.

As will be seen below, these treatments lead to different predictions of conformational variablitity of the four-way junction. The different distant-dependent variations of ϵ fit into two broad categories, one where ϵ increases gradually (eq 4, $\epsilon = r_{ij}$, and the Debye–Hückel treatment) and the other (eqs 3 and 5) with a sharp transition at some critical distance. While the individual schemes have previously proven useful in specific contexts (see citations above), it is not yet clear if any is totally satisfactory in accounting for the electrostatic interactions of nucleic acids. Hence all available potentials are considered here.

Four-Way Junction. If a phosphorus atom is successfully placed between nucleosides l and m′, a cross-link L_{12} is said to have been established, and the potential energy of the resulting dG_l-p-$dG_{m'}$ dinucleoside monophosphate is computed. Similarly, a search is made to locate a phosphorus atom between nucleosides l′ and m for the same three-dimensional interhelical arrangement. Successful completion of this process leads to the establishment of a cross-link, L_{21}. Following this, the potential energy of the dinucleoside monophosphate $dG_{l'}$-p-dG_m is determined.

For a given relative orientation of DNA1 and DNA2, because of the allowed variation in the glycosyl torsions, sugar puckering, and choice of C5′–C4′ torsion angles (ψ_1 and ψ_2), numerous pairs of cross-links may exist. Each unique set of interhelical arrangements $\{\theta, \theta1, \theta2, \Delta x, \Delta y, \Delta z\}$ is termed a helical placement, H_p. In order to form a four-stranded junction, the helical placement must be the same for both interduplex cross-links. The H_p values tabulated below correspond to the number of distinct helical arrangements common to the L_{12} and L_{21} crossover sites for a given azimuthal orientation, θ. The number of potential four-way junctions ($J^\dagger_4$) at each θ is thus much less than the product $L_{12} \times L_{21}$ (see below). The value of $J^\dagger_4$ is computed from subsets of crossover links (termed L_{12}' and L_{21}') at each helical placement (specifically the sum of the $L_{12}' \times L_{21}'$ over all common combinations of $\{\theta1, \theta2, \Delta x, \Delta y, \Delta z\}$ at fixed θ). An arbitrary intra-strand energy limit of 10 kcal mol^{-1} (absolute energy) is imposed on the $J^\dagger_4$ before counting them as preliminary four-way junctions. Also, for ease of generating four-stranded Holliday junctions, a local pair is further considered only when the glycosyl torsions and the sugar puckers in both crossover linkages match those in one of the B-DNA helices listed in the Appendix. These additional restrictions eliminate a number of the potential four-way links, leaving a partial set for further analysis. Each of the restricted local pairs in this partial set (called J^*_4) corresponds to an energetically stable dinucleoside monophosphate conformer (either dG_l-p-$dG_{m'}$ or $dG_{l'}$-p-dG_m).

The simultaneous generation of a pair of cross-links with the above-mentioned torsional and energetic constraints suggests the successful construction of a crossover between the interacting G-strands of DNA1 and DNA2. To test this possibility, the nonbonded pairwise interaction energy (both intra- and interstrand contributions) of each local junction is computed using standard potential functions and constants (Srinivasan *et al.*, 1987). All local junctions less than an absolute energy limit of 100 kcal mol^{-1} are accepted as feasible crossover sites within an extended four-way helical junction. The number of these states, each of which corresponds to an energetically stable dinucleoside monophosphate complex (dG_l-p-$dG_{m'}$ and $dG_{l'}$-p-dG_m), is compiled as J_4 below.

As a final step, extended four-way helical models are constructed by introducing the appropriate low-energy local four-way junctions between DNA molecules oriented in a given interhelical arrangement. The overall stability of the extended junctions is then estimated by computing the nonbonded interactions within the entire structure using the various formulations outlined above.

Table 1: Total Number of Backbone Linkages as a Function of Interhelical Azimuthal Angle θ at Various Stages of Modeling DNA Four-Way Junctions

	single-strand links		spatial matches	four-way junctions		
θ (deg)	L_{12}	L_{21}	H_p	$J^\dagger_4$	J^*_4	J_4
±180	24 224	21 770	600	54 530	7548	43
−135	20 490	19 251	737	55 390	6800	312
−90	15 616	16 491	629	29 093	3902	307
−45	19 791	20 386	1022	40 089	5422	620
0	20 785	20 108	622	58 262	7867	539
45	25 157	22 960	583	69 885	8901	322
90	24 528	21 508	430	61 305	7913	12
135	26 674	24 481	477	72 850	9648	0

RESULTS

As described above, strand crossovers are first examined at the local single-stranded level. The energetically favorable conformers are then included in preliminary models of higher order four-way DNA junctions. Holliday structures with arms of roughly one helical turn are constructed only if the local crossover geometry (*i.e.*, intra- and interstrand energy) is deemed acceptable.

Single-Strand Crossover Structures. The number of single-stranded backbone conformations with acceptable valence angle geometry forming crossover links L_{12} and L_{21} between DNA helices at various azimuthal orientations is listed in Table 1. The total number of covalent linkages between residues l and m′ (L_{12}) and l′ and m (L_{21}) is roughly the same order of magnitude. These backbone conformers, however, represent only a small fraction of the total number of spatial states considered in the search (specifically, 0.054% for L_{12} and 0.051% for L_{21} of the 329 801 472 configurations arising from the $8 \times 13 \times 13 \times 7 \times 11 \times 11 \times 36 \times 4 \times 2$ respective combinations of θ, $\theta1$, $\theta2$, Δx, Δy, Δz, ψ, χ, and P per single-stranded dimer step). At this stage of the calculations, there is no significant preference for one interhelical orientation over another; roughly 2×10^4 single-stranded states are found at each value of θ for either crossover linkage.

The number of unique interhelical placements H_p corresponding to each θ is reported in the fourth column of Table 1. The greatest number of placements (1022) is found for $\theta = -45°$ and the lowest number (430) for $\theta = 90°$. All together, there are ~5100 distinct spatial combinations that lead to interstrand chemical linkages between single-stranded nicks in closely packed B-DNA duplexes. Interestingly, the number of helical matches drops roughly in half when the two DNAs are reoriented from $\theta = -45°$ to $\theta = 45°$. The orientation of helices in these two states, which differ in directionality or handedness of the constituent chain segments, resembles the (~60°) X-like packing of DNA observed in recent B-DNA

Table 2: Local Base Morphology of DNA Four-Way Junctions and Related Crystal Structures as a Function of Interhelical Orientation

helical disposition						local base morphology						
θ (deg)	$\theta 1$ (deg)	$\theta 2$ (deg)	Δx (Å)	Δy (Å)	Δz (Å)	tilt (deg)	roll (deg)	twist (deg)	shift (Å)	slide (Å)	rise (Å)	related crystal
±180	−15 ± 12	−21 ± 12	−17 ± 1	0 ± 3	1 ± 1	0 ± 0	180 ± 0	179 ± 15	−5 ± 1	8 ± 0	1 ± 1	
						0.4	−160.0	150.5	−4.9	5.7	4.7	dCGCGCGTTTTCGCGCG[a]
−135	−28 ± 18	−9 ± 20	−19 ± 1	−1 ± 3	2 ± 3	−4 ± 12	−137 ± 2	−154 ± 29	−8 ± 3	8 ± 1	2 ± 1	
						2.2	154.2	−114.0	−8.6	7.7	−3.0	dCGCAGAATTCGCG[b]
						6.6	161.5	−149.1	−7.0	9.0	−3.3	dCGCAGAATTCGCG[b]
						6.9	178.4	−90.6	−9.5	5.0	−6.2	ApA·proflavin[c]
−90	−41 ± 15	6 ± 18	−19 ± 1	0 ± 3	0 ± 3	7 ± 15	−90 ± 0	−136 ± 18	−10 ± 2	8 ± 1	3 ± 2	
−45	−41 ± 14	5 ± 15	−20 ± 1	0 ± 3	0 ± 2	5 ± 10	−44 ± 1	−141 ± 16	−10 ± 2	7 ± 1	3 ± 2	
						−31.6	−43.0	−172.7	−6.4	8.1	4.8	dGpdC·actinomycin[d]
0	−38 ± 16	6 ± 20	−19 ± 1	−1 ± 3	0 ± 1	0 ± 0	0 ± 0	−140 ± 31	−11 ± 2	5 ± 3	3 ± 1	
						−3.5	10.0	−85.4	−6.7	4.1	5.9	UpA-2[e]
						−1.8	8.2	−86.1	−6.7	4.1	5.9	UpA-2′[f]
						13.1	1.8	−133.8	−8.3	6.9	−1.0	dCGCAGAATTCGCG[b]
45	−43 ± 14	−10 ± 20	−19 ± 1	0 ± 3	0 ± 3	−7 ± 10	44 ± 1	−138 ± 24	−12 ± 1	4 ± 2	2 ± 1	
90	−40 ± 10	−20 ± 0	−18 ± 0	−1 ± 2	−5 ± 0	−7 ± 10	90 ± 0	−161 ± 0	−11 ± 0	6 ± 0	1 ± 1	
						−6.4	108.9	−178.5	−4.6	7.5	3.2	aa stem yeast $tRNA^{Phe}$[g]
						20.3	129.0	179.0	−3.4	8.1	1.5	D-loop yeast $tRNA^{Phe}$[g]

[a] Chattopadhyaya *et al.*, 1988. [b] Joshua-Tor *et al.*, 1992. [c] Neidle *et al.*, 1978. [d] Takusagawa *et al.*, 1982. [e] Seeman *et al.*, 1971. [f] Rubin *et al.*, 1972. [g] Robertus *et al.*, 1974; unusual dimer steps in longer oligomers are underlined.

single-crystal structures (Timsit *et al.*, 1989, 1991; Heinemann *et al.*, 1992; Baikalov *et al.*, 1993; Lipanov *et al.*, 1993). The fluorescent properties of four-stranded oligonucleotides, however, suggest that the helical arms are oriented at angles closer to antiparallel than parallel (*i.e.*, ±120° *vs* ±60° according to our definition) in solution (Murchie *et al.*, 1989).

The total number of potential four-way links ($J^{\dagger}_4$) found for each azimuthal orientation without consideration of local energy or chain conformation, as detailed above, is reported in the fifth column of Table 1. The fewest possibilities occur at $\theta = -90°$ and the most at $\theta = 135°$. The number of local matches is roughly the same for antiparallel ($\theta = \pm 180°$) and parallel ($\theta = 0°$) duplex alignments (54 530 and 58 262, respectively) but is quite different for opposing perpendicular placements of helices (61 305 for $\theta = 90°$ and 29 093 for $\theta = -90°$).

Reported in the last two columns of Table 1 is the number of local four-way junctions that meet energetic and conformational criteria within each linking strand (J^{*}_4) and of those that satisfy additional interstrand energy constraints (J_4) for all eight azimuthal orientations of DNA duplexes. As noted above, each strand of a local junction must be less than 10 kcal mol^{-1} absolute energy and must also adopt the identical sugar puckering and glycosyl torsion as the B-DNA helical arm to which it is attached. On average, 87% of the potential junctions (*i.e.*, the $J^{\dagger}_4$) observed from simply counting the number of links with common helical placements are eliminated by these criteria (compare the fifth and sixth columns in the table), leaving a total of 58 001 local junctions with acceptable intrastrand backbone linkages (J^{*}_4) over all interhelical arrangements and 2155 with acceptable intra- and interstrand contacts (J_4). The significant reduction in J_4 compared to J^{*}_4 stems, in large part, from unfavorable interstrand steric clashes between phosphate side-group oxygens on the two crossover linkages. The greatest number of local four-way junctions meeting all energetic and conformational criteria is found at $\theta = -45°$. Surprisingly, there are no acceptable local four-way models with DNAs oriented at an angle of $\theta = 135°$ despite the highest preference for this orientation of double helices on the basis of intrastrand energy and conformation (*i.e.*, 9648 J^{*}_4 states).

Optimized Four-Way Local Junctions. The three-dimensional conformations of DNA identified in the search of local four-way junctions are quite different from the standard arrangements of bases and backbone within the double helix. One of the easiest ways to understand the unusual chain folding at the crossover sites is in terms of the relative positioning of linked bases (1 to m′ and 1′ to m). The sets of rotational angles (tilt, roll, twist) and translational parameters (shift, slide, rise) listed in Table 2 for all energetically stable local junctions should be compared against the corresponding base morphology of the idealized B-DNA duplexes, with angles of (0°, 0°, 36°) and displacements of (0 Å, 0 Å, 3.4 Å). The numerical values characterizing the various junctions in Table 2 are the mean and standard deviations of adjacent base parameters in the final low-energy (J_4) crossover sites for each azimuthal placement. As is immediately obvious from the data, the only spatial similarity between the B-DNA duplex and the low-energy junctions lies in the tilt angle, which fluctuates at levels dependent upon the interhelical placement around 0°. The local twist at the crossover site, while also restricted to a single range, varies around atypical values near ±180°. The standard deviations of tilt and twist are noticeably larger than those of roll at each value of θ. The average roll angle, however, shows a striking correlation with azimuthal placement, being roughly equivalent to the value of θ. Smooth interconversion from one kind of junction to the next can thus occur by simply bending the chains in the direction of the major or minor grooves of the flanking helices. This finding is consistent with the known tendencies of double-helical DNA to bend preferentially along the roll rather than the tilt coordinate (Ulyanov & Zhurkin, 1984; Srinivasan *et al.*, 1987; Sarai *et al.*, 1989; Grzeskowiak *et al.*, 1993). The displacement of bases, measured laterally by shift and slide and vertically by rise, is naturally much larger at the crossover sites than in the double helix. The mean center-to-center distance of neighboring base pairs at the four-way junction ranges from 9.5 to 13.2 Å, depending upon interhelical placement.

Also reported in Table 2 is the rough morphological similarity of bases in the theoretically generated four-way junctions with residues exhibiting unusual base stacking in various single-crystal nucleic acid structures. Some of the structures are specifically labeled as unusual in the Nucleic Acid Database (Berman *et al.*, 1992), while others have been identified on the basis of unusual features in selected helical structures. The examples span the gamut from free and drug-

Table 3: Minimum Energy Conformations[a] and Energy[b] of DNA Four-Way Junctions as a Function of Azimuthal Orientation

			L_{12} crossover					L_{21} crossover					
θ (deg)	χ	P	ϕ_1' C3′—	ω_1' O3′—	ω_1 P—	ϕ_1 O5′—	ψ_1 C5′— C4′	ϕ_2' C3′—	ω_2' O3′—	ω_2 P—	ϕ_2 O5′—	ψ_2 C5′— C4′	E (kcal mol^{-1})
Local Four-Base-Pair Junction													
±180	a	^{2}E	g^-	g^-	g^-	g^-	g^+	g^-	t	g^+	g^+	g^-	−89.7 (−89.7)
−135	a	^{2}E	g^-	g^-	g^-	g^-	g^+	g^-	t	t	g^-	g^+	−82.4 (−83.2)
−90	a	^{2}E	g^-	t	g^+	g^+	g^-	g^-	g^+	t	g^+	g^-	−81.0 (−82.0)
−45	a	^{2}E	g^-	g^-	t	g^-	g^-	g^-	g^+	t	g^+	g^-	−81.9 (−83.9)
0	a	^{2}E	g^-	g^+	g^+	g^+	g^-	g^-	g^-	t	g^-	g^-	−83.2 (−83.2)
45	a	^{2}E	t	g^-	t	t	g^-	t	g^+	g^+	g^+	g^-	−73.2 (−81.0)
90	a	^{2}E	t	t	g^-	t	g^-	t	t	g^+	t	t	17.0 (−26.2)
Helical Four-Way Junction													
±180	a	^{2}E	g^+	t	g^+	t	g^-	g^-	g^-	g^-	t	g^+	53.9 (53.9)
−135	a	^{2}E	g^-	g^-	g^-	t	g^-	g^-	g^-	g^-	t	g^+	36.6 (35.0)
−90	a	^{2}E	g^-	t	g^+	g^+	t	g^-	g^+	t	g^+	g^-	67.3 (65.0)
−45	a	^{2}E	g^-	g^+	t	g^+	g^-	g^-	g^-	t	t	g^-	57.6 (53.5)
0	a	^{2}E	g^-	t	t	g^+	t	t	t	t	g^+	g^-	71.6 (71.6)
45	a	^{2}E	t	g^-	t	t	g^-	t	g^+	g^+	g^+	g^-	45.2 (37.0)
90	a	^{2}E	t	t	g^-	t	g^-	t	t	g^+	t	t	154.0 (110.6)

[a] Acyclic torsions are classified in terms of conformational range: *trans* (t = +180 ± 60°); *gauche*$^\pm$ ($g^\pm$ = ±60 ± 60°). [b] Energies correspond to the mean overall states and the minimum (in parentheses) for the given conformational family.

bound dinucleoside monophosphates (Seeman *et al.*, 1971; Rubin *et al.*, 1972; Neidle *et al.*, 1978; Takusagawa *et al.*, 1982) to longer chains with hairpin loops and/or single-stranded unpaired bases (Robertus *et al.*, 1974; Chattopadhyaya *et al.*, 1988; Joshua-Tor *et al.*, 1992). The modeling points to a potential new role for the unusual backbone conformations observed experimentally, while the correspondence between predicted and solved structures provides an added measure of confidence in the computational approach. The agreement between theory and experiment, nevertheless, is quite crude with none of the observed solid-state structures precisely overlapping any of the predicted four-way junctions. The specific base-pair steps and literature references are noted at the appropriate values of θ in the table. Rough similarities to known crystal structures are found for six of the eight types of four-way junctions. Considering the fact that the computed models are obtained from an arbitrary choice of base-pair positions and a wide conformational search, the agreement with solid-state data is significant.

Table 3 provides additional structural features of the local four-way junctions. The upper half of the table lists the backbone conformations and energy values of the lowest energy states found at different azimuthal orientations (*i.e.*, the mean values for the energetically most favored conformational family among the accepted J_4 states at a given θ). The acyclic torsions are classified in terms of conformational range [*i.e.*, *trans* (t = ±180 ± 60°) or *gauche*$^\pm$ ($g^\pm$ = ±60 ± 60°)], while the glycosyl torsion is *anti* (*a*) and the sugar puckering C2′-endo (^{2}E) in all cases. Backbone torsions labeled with subscript 12 correspond to the dG_l-p-$dG_{m'}$ crossover and those with subscript 21 to the $dG_{l'}$-p-dG_m linkage. Conformationally identical linkages are divided into groups, and the average absolute energy of all states in the groups is determined. The energies E are the numerical values obtained by summing the nonbonded intra- and interstrand interactions of atoms on the two single-stranded links (*i.e.*, all possible pairwise combinations of atoms on links L_{12} and L_{21}). Also listed in the table are the minimum energy values for each of the conformational families (in parentheses in the last column). Except for the junction with helices oriented at an angle θ of 90°, all of the minimum energy forms are of comparable energy (according to both mean and minimum energy values). The higher average energy of the θ = 90° state is presumably related to the highly stretched backbone with fully extended *trans* torsional states in this arrangement.

Stereoviews of the seven "minimum" energy crossover structures (noted in parentheses in Table 3) with the corresponding interhelical orientation angle θ are presented in Figure 4. These energy "minima" are conformations with the least energy among the various structures of a given type and should not be confused with the results of a standard energy minimization. The interactions of sugar rings appear to be the same on the right sides of the junctions (originally part of DNA1) but to vary with changing θ on the left sides. The stacking of bases between exchanged strands, however, is the same over the complete range of azimuthal orientations. Interestingly, pendant phosphate oxygens on the two backbone strands face in opposite directions in all structures in the figure. This sort of arrangement, with little interstrand steric hindrance, may facilitate conformational transitions from one orientational state to another at a given crossover site as well as possibly ease smooth migration of exchanged strands along the DNA. Specific bonding constraints of associated cations with the phosphate group, which are not considered here, could change this picture. Terminal O3′–C3′ bonds on the two dinucleoside monophosphate units and terminal C4′–C5′ bonds on the two low-energy backbones also point in opposite directions in the low-energy four-way junctions. Residues can thus be added to either side of the four-way local junction with little, if any, steric clash. The spatial disposition (*i.e.*, $\theta 1$, $\theta 2$, Δx, Δy, and Δz) of the successfully linked helices in each of the minimum energy local junctions is reported in the upper half of Table 4. The positioning of helices in these specific states is not necessarily the same as the mean parameters reported in Table 2. The general arrangement of helices, nevertheless, holds for all low-energy four-way models, including the different energy minima. For example, in all the cases but one ($\theta = \pm 180°$) in Tables 2 and 4, the difference $\theta 1 - \theta 2$ is negative, indicating a negative screw rotation between duplexes at the four-way DNA junctions. The interhelical separation measured by Δx is also relatively constant in all crossover structures, while there is larger variation (up to 10 Å) in both the helix axis offset Δy and the vertical slippage Δz of duplex arms in the local junctions.

Extended Four-Way Helical Junctions. In order to estimate the conformational preferences of naturally occurring Holliday junctions, we have built extended four-stranded helical complexes (with 10 bp per duplex arm) corresponding to all

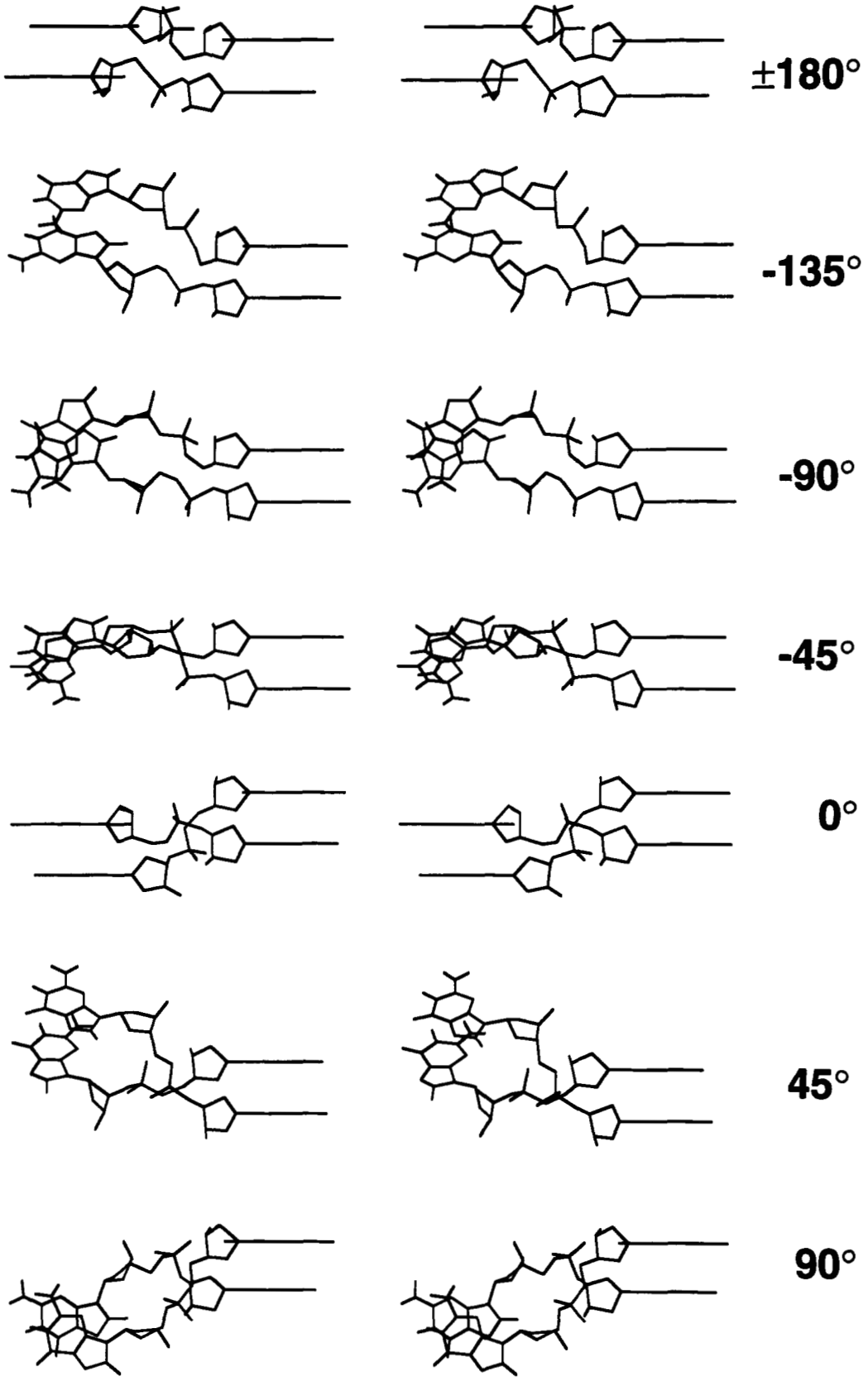

FIGURE 4: Stereoviews (Chem-X, Chemical Design Inc.) of local minimum energy crossover structures as a function of interhelical orientation angle θ.

spatially matched, low-energy local junctions (*i.e.*, the 2155 J_4 states in Table 1) and have calculated nonbonded interactions between atoms and phosphate groups in the resulting structures. Each large-scale model is constructed by first orienting two 20-bp DNA duplexes (DNA1 and DNA2) with spatial parameters corresponding to the local crossover models (J_4) and removing the O5′, P, O1, and O2 atoms between bases G_l and G_m of DNA1 and $G_{l'}$ and $G_{m'}$ of DNA2. The positions of the corresponding atoms in the four-way local junction are then introduced in the helical model. The nonbonded distances between all atom pairs whose interatomic separation changes with θ are subsequently computed and

Table 4: Spatial Rotations and Displacements of Exchanged Helices of Low-Energy DNA Four-Way Junctions as a Function of Interhelical Orientation Angle

θ (deg)	θ1 (deg)	θ2 (deg)	Δx (Å)	Δy (Å)	Δz (Å)
		Four-Way Local Junction			
±180	−30	−40	−17	5	1
−135	−40	−20	−19	3	4
−90	−50	0	−20	3	2
−45	−50	20	−20	4	0
0	−40	−20	−19	−5	−2
45	−50	40	−18	5	5
90	−30	−20	−18	−2	−5
		Extended Four-Way Helical Junction			
±180	−10	−10	−18	−2	0
−135	0	−40	−16	−1	5
−90	−60	0	−19	5	2
−45	−40	10	−20	1	−3
0	−30	0	−20	−4	0
45	−50	40	−18	5	5
90	−30	−20	−18	−2	−5

introduced in the different potential energy schemes.

The backbone and glycosyl torsions, sugar puckering, and all-atom energy of the lowest energy extended helical junctions at each azimuthal orientation are listed in the lower half of Table 3. The extended four-way helical junctions are divided into groups of conformationally identical J_4 states, and the average absolute energies of all states within the groups are determined. The energies in the table correspond to the mean and absolute minimum for the most favored conformational family at each θ. The backbone connections in most of the optimized helical models are different from those found to be of lowest energy at the local level, with an exact match of torsional ranges occurring only for complexes where θ = 90° and 45°. Long-range contacts present in the extended junctions tend to reorder and sometimes exclude the low-energy local states. The relative spatial disposition of interacting helices in the minimum energy extended models is thus somewhat different from those of the local junctions, again except for the θ = 90° and 45° states (see Table 4). The significantly higher energies of the helical versus local four-way junctions (Table 3) reflect the added phosphate repulsions in the larger system. Both sets of molecules in Table 3 are treated with a fixed dielectric constant of 4. Interestingly, helical models resembling an X-shape (θ = −135° or 45°) are lower in energy than other arrangements of crossed duplexes at this level of approximation. These states, respectively related to the crossed arrangements of double helices in synthetic junctions (Cooper & Hagerman, 1987, 1989; Churchill *et al.*, 1988; Duckett *et al.*, 1988; Murchie *et al.*, 1989) and certain crystalline models (Timsit *et al.*, 1989, 1991; Heinemann *et al.*, 1992; Baikalov *et al.*, 1993; Lipanov *et al.*, 1993), are stabilized by favorable van der Waals contacts between atoms on the interdigitated duplex arms. A large number of atom pairs fall at or near their optimum separation distances in these configurations, generating a near-perfect fit of the two halves of the DNA. Nevertheless, the packing of helices in the θ = −135° state is also similar to that found in the interwound equilibrium arrangements of long elastic supercoils (Hao & Olson, 1989; Zhang *et al.*, 1991; Schlick & Olson, 1992; Yang *et al.*, 1993). Moreover, the negative strand crossing [obtained by the standard mathematical definition (White, 1989)] is typical of that brought about by a linking number deficit in naturally occurring supercoils (Cozzarelli *et al.*, 1990). The crossing geometry characteristic of an overwound DNA supercoil (θ = 135°) is not found to lead to an energetically acceptable four-way structure. As pointed out by a referee, this attraction between helical arms may be less strong in solvated models of DNA.

The seven minimum energy Holliday models are illustrated in color from two perspectives in Figure 5. One view shows the azimuthal rotation of duplex arms out of the plane of the figure and the other the relative angular motions in the plane of the page. The two exchanged single strands are depicted by space-filling models, the DNA1 → DNA2 strand with the dG_l-p-$dG_{m'}$ crossover in red and the DNA2 → DNA1 strand with the $dG_{l'}$-p-dG_m crossover in gold. The unexchanged strands of the original duplexes are shown in white, the DNA1 strand on the right in Figure 5a and in the back in Figure 5b. Note the close contacts of unexchanged strands in the θ = 0°, 45°, ±180°, −135°, and −45° configurations and the potential for additional exchange of DNA between these chains. Examination of the P···P contact distances in these models reveals that the uncrossed white strands approach each other within 6 Å in the θ = 0°, ±180°, and −45° cases. However, a detailed analysis of the P···P contacts in all the low-energy conformations (<100 kcal mol^{-1} above the absolute minimum) indicates that other crossed forms (namely, θ = 45° and −135°) also show this feature. With longer antiparallel (θ = ±180°) and parallel (θ = 0°) junctions, there is the possibility of exchange between the same strands at different sites on the two DNAs. Close nonbonded contacts repeat after integral turns of the associated helices. Such exchange at θ = ±180° could lead to a series of closed circular single strands interlaced by unexchanged single helices and at 0° to a four-stranded interweaving of polynucleotide chains. The repeated exchange sites in the antiparallel (θ = ±180°) arrangements are critical features of the double crossover DNA molecules recently synthesized by Fu and Seeman (1993). The secondary contacts between unexchanged strands have been exploited in the design of these compounds.

Conformational Flexibility. The molecular models constructed in this study provide rough estimates of the relative conformational stabilities and flexibility of four-way double-helical DNA junctions. The series of configurations in Figure 5 is suggestive of potential large-scale conformational transitions involving four-way DNA junctions. The compilation of long-range electrostatic energies in Table 5 gives some hint of this flexibility. The numerical values correspond to the lowest energy state found for all junctions with a given azimuthal orientation of helical arms according to the specified dielectric treatment. These states do not necessarily fall in the most favored conformational families listed in Table 3. Data are reported for both all-atom and P-atom representations of the junctions with the net charge per nucleotide residue (−0.22 esu) concentrated on the phosphorus positions in the latter cases (reported in parentheses). The interhelical orientations of lowest absolute energy for each energy treatment are highlighted in boldface.

As evident from Table 5, the ranking of spatial configurations is altered with different dielectric models in the all-atom calculations. For example, the lowest energy form occurs at θ = 45° if ε is set to the dielectric constant of water, modeled by the Debye–Hückel equation, or treated with the sigmoidal distance-dependent dielectric functions of Hingerty *et al.* (eq 3) and Mazur and Jernigan (eq 5 with p = 1 or 2) but is shifted to θ = −135° if ε is set equal to 4, approximated by the interatomic distance, or represented by the distance-dependent dielectric function of Lavery *et al.* (eq 4). The three latter dielectric treatments place more importance on close-range electrostatic interactions than the former schemes (*i.e.*, ε is either very low or a more slowly increasing value in

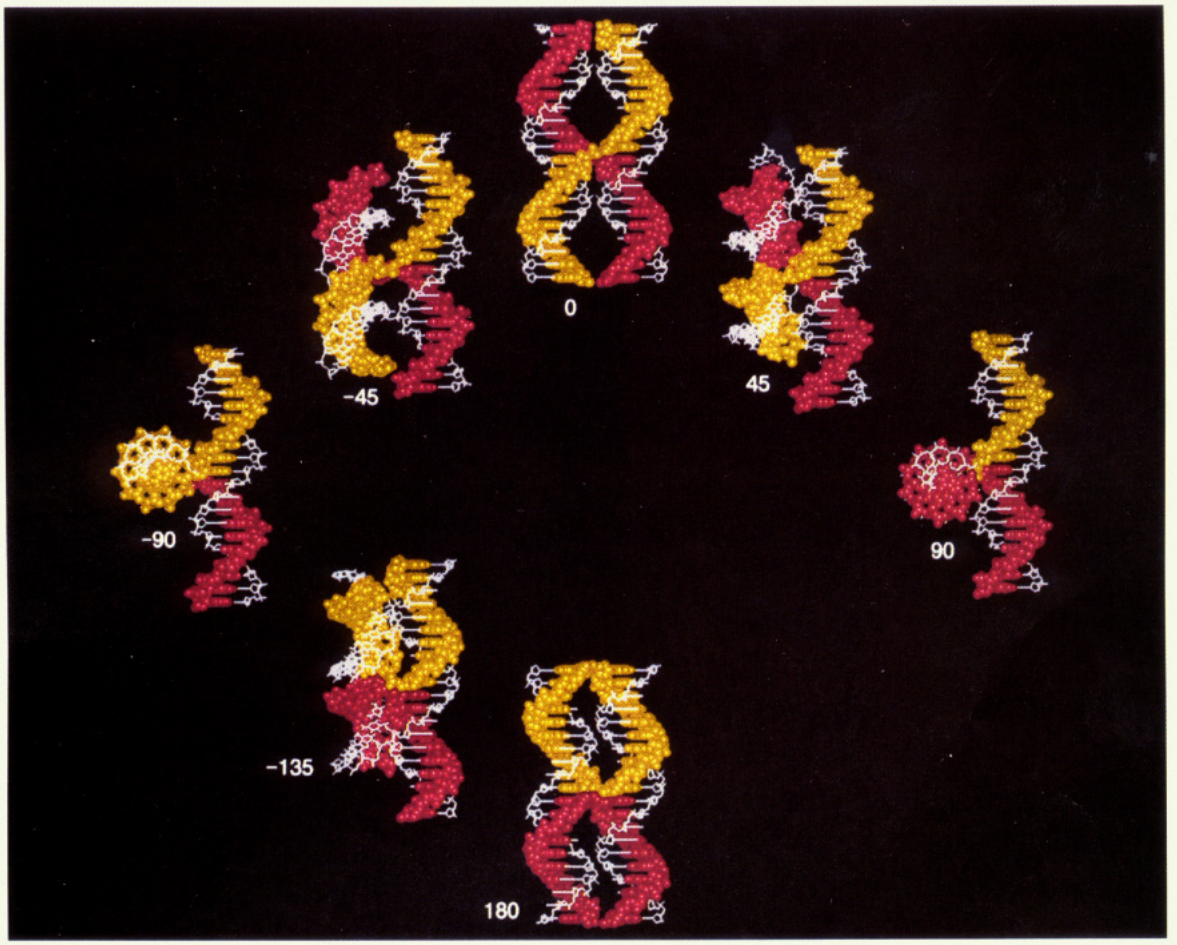
0
-45
45
-90
90
-135
180


0
-45
45
-90
90
-135
180

Table 5: Minimum Nonbonded Energies (in kcal mol^{-1}) of Extended Holliday Junctions for Different Azimuthal Orientations of Helical Arms under Different Dielectric Treatments[a]

							eq 5		
θ (deg)	$\epsilon = 4$	$\epsilon = \epsilon_\infty$	$\epsilon = r_{ij}$	$\epsilon = \epsilon_\infty \exp(r_{ij}/D)$	eq 3	eq 4	$p = 1$	$p = 2$	6–12[b]
±180	53.9	82.9	−38.5	79.9	55.4	−150.4	69.1	68.9	84.6
	(490.5)	(25.2)	(117.6)	(4.2)	(30.9)	(78.4)	(33.7)	(28.0)	
−135	**24.4**	−14.8	**−81.0**	−19.4	−31.4	**−181.5**	−22.4	−23.7	−16.9
	(467.4)	(24.0)	(104.0)	(3.7)	(28.0)	(61.4)	(31.4)	(26.0)	
−90	58.9	−12.8	−67.6	−18.7	−27.8	−162.0	−19.3	−21.0	−16.7
	(460.0)	**(23.6)**	**(100.8)**	**(3.5)**	**(27.6)**	**(60.2)**	**(30.7)**	**(25.5)**	
−45	34.9	−13.9	−70.5	−19.2	−27.2	−167.2	−20.3	−20.5	−6.5
	(464.4)	(23.8)	(103.4)	(3.6)	(28.0)	(62.3)	(31.2)	(25.9)	
0	46.0	3.2	−56.2	−1.5	−10.6	−126.9	−3.5	−3.9	1.0
	(477.5)	(24.5)	(112.1)	(4.0)	(29.9)	(73.9)	(32.7)	(27.3)	
45	29.7	**−21.3**	−76.2	**−26.3**	**−33.5**	−126.4	**−27.5**	**−27.2**	−23.4
	(469.5)	(24.1)	(105.1)	(3.7)	(28.2)	(62.4)	(31.5)	(26.1)	
90	110.6	52.4	−6.0	47.0	38.0	−81.0	45.7	45.0	49.2
	(470.1)	(24.1)	(105.4)	(3.7)	(28.4)	(63.3)	(31.6)	(26.2)	

[a] Configurations are the helical four-way junctions of lowest energy at the specified azimuthal orientation. The orientation of lowest absolute energy for each treatment is noted in boldface. Minimum electrostatic energies between P atoms (net charge −0.22 esu per nucleotide) are given in parentheses; $\epsilon_\infty = 78$. [b] The van der Waals contribution to the total energy.

the last three cases). The first five treatments reproduce the crossed parallel packing of DNA duplexes in the crystal, while the latter models account successfully for the apparent antiparallel form of four-way oligonucleotide junctions in solution and the packing of associated duplexes in interwound supercoils. The different forces stabilizing one configuration over the other may thus be mimicking the different electrostatic environments in the solid state and in solution. The predicted differences between the two kinds of minima (45° and −135°) are, nevertheless, fairly small for all but one (eq 4) of the all-atom calculations. Notably, the minimum energy states are X-shapes regardless of dielectric model. As might be expected from the extensive contacts of phosphate groups, the highest all-atom and phosphate energies consistently occur when the duplexes are in perfect antiparallel ($\theta = \pm 180°$) or parallel ($\theta = 0°$) alignment. As further expected from their greater average pairwise separation, the repulsions of P atoms are lowest when the arms of the four-way junction are perpendicular (specifically $\theta = -90°$). The apparent preference for X arrangements over "square-planar" forms in solution and in the solid state again points to the potential importance of van der Waals–London interactions in stabilizing Holliday junctions.

The van der Waals energy contributions to the low-energy four-way junctions are listed in the last column of Table 5 (the data at $\theta = -45°$ and $\theta = 45°$ are averages reflecting several different low-energy conformations predicted by specific electrostatic potentials). The numerical values are relatively high for the models formed at the extremities of the conformation space probed in this study (*i.e.*, $\theta = 90°$ and $\theta = 180°$) . The limiting conformation corresponding to $\theta = 90°$, as seen from Figure 4, necessitates highly "stretched" sugar–phosphate backbones at the crossover site, whereas backbone "compression" is apparent in the $\theta = 180°$ model. These steric limitations reveal why we cannot build four-way junction models at $\theta = 135°$ (which is outside these extremes). The low van der Waals energies of the intermediate forms of the junction ($\theta = -135°$, −90°, −45°, 0°, and 45°) suggest that these conformations may be stabilized by van der Waals contributions. It is noteworthy that most of these states are crossed orientations.

The many low-energy states identified in the model building scheme provide additional measures of the configurational preferences of the Holliday model. The number of low-energy states with a given placement of duplex arms can be used as a rough estimate of the configurational entropy of the different azimuthal arrangements. In view of the very crude sampling of conformational states and the approximate nature of the potential energy functions used here, all four-stranded extended helical models within 25 kcal mol^{-1} of the absolute minimum for each dielectric treatment are counted equally. The sum of such states at each azimuthal orientation, $J_H(\theta)$, is then used to estimate the configurational entropy as $\ln J_H(\theta)$. The relative preferences of the various arrangements of duplex arms are presented as unitless relative values in Table 6 for the different energy treatments. The most populous states are perpendicular and/or crossed configurations regardless of energy treatment or atomic model. These states are subject to fewer steric contacts and weaker electrostatic repulsions than configurations with helical arms aligned side by side in the same or opposing direction. There is a greater tendency for the helical arms to align in parallel ($\theta = 0 \pm 45°$) if only phosphorus atom repulsions are treated, whereas antiparallel ($\theta \sim 180°$) configurations occur with roughly comparable frequency if all atoms are considered. The $\theta = -135°$ crossed state most closely resembling the interwinding of helices in supercoiled DNA and the geometry of four-way junctions in solution is the most highly populated state in several energy treatments. The same trends in conformational populations also persist if different energy cutoffs (10 and 50 kcal mol^{-1}) are considered.

DISCUSSION

Conformational Variability. The wide range of branched DNA structures identified through constrained model building shed new light on the preferred conformations of the Holliday junction and the likely pathways involved in branch migration. Our systematic survey of duplex association and interhelical strand exchange yields conformationally acceptable molecular models with double-helical arms oriented over a 270° range of values. The predicted four-arm structures include the antiparallel uncrossed form inferred from solution studies and

FIGURE 5: Color-coded representation (InsightII, BIOSYM Technologies) of low-energy Holliday models of DNA strand crossover as a function of interhelical orientation angle θ. The DNA1 → DNA2 exchanged strand with the dG_l-p-$dG_{m'}$ crossover is shown in red and the DNA2 → DNA1 exchanged strand with the $dG_{l'}$-p-dG_m crossover in gold. The unexchanged strands of the original duplexes are shown in white: (a, top) view in the same direction as in Figure 4 illustrating the azimuthal rotation of DNA2 out of the plane of the paper; (b, bottom) view obtained by rotating the complex 90° about the helical axis of DNA1 to illustrate the range of crossings of duplex arms.

Table 6: Estimated Configurational Entropy of Extended Holliday Junctions with Different Azimuthal Orientations of Helical Arms as a Function of Dielectric Treatment[a]

							eq 5	
θ (deg)	$\epsilon = 4$	$\epsilon = \epsilon_\infty$	$\epsilon = r_{ij}$	$\epsilon = \epsilon_\infty \exp(r_{ij}/D)$	eq 3	eq 4	$p = 1$	$p = 2$
±180	0.0	0.0	1.1	0.0	0.0	2.6	0.0	0.0
	(0.0)	(0.0)	(0.0)	(3.8)	(0.0)	(0.0)	(0.0)	(0.0)
−135	0.0	4.6	**5.4**	**4.8**	4.9	**5.6**	4.8	4.8
	(0.0)	(5.4)	(0.0)	(5.7)	(0.0)	(0.0)	(0.0)	(0.0)
−90	0.0	4.6	5.2	**4.8**	**5.0**	5.4	4.8	**4.9**
	(0.0)	(5.7)	(0.0)	(5.7)	(0.0)	(0.0)	(0.0)	(0.0)
−45	0.0	**4.8**	5.3	**4.8**	4.9	**5.6**	**4.9**	**4.9**
	(0.0)	(**6.3**)	(0.0)	(**6.4**)	(0.0)	(0.0)	(0.0)	(0.0)
0	0.0	0.0	1.6	0.0	0.7	3.1	0.0	0.0
	(0.0)	(5.5)	(0.0)	(6.3)	(0.0)	(0.0)	(0.0)	(0.0)
45	0.0	4.0	5.0	4.2	4.4	5.4	4.1	4.2
	(0.0)	(5.8)	(0.0)	(5.8)	(0.0)	(0.0)	(0.0)	(0.0)
90	0.0	0.0	0.0	0.0	0.0	1.4	0.0	0.0
	(0.0)	(2.5)	(0.0)	(2.5)	(0.0)	(0.0)	(0.0)	(0.0)

[a] Configurational entropy is given by $\ln J_H(\theta)$, where $J_H(\theta)$ is the number of distinct states within 25 kcal mol^{-1} of the minimum energy configuration of an extended four-way junction with specified azimuthal orientation of helical arms. The orientational state of greatest potential flexibility for a given energy treatment is noted in boldface. Data based on electrostatic energies of P atoms (−0.22 net charge per nucleotide) are given in parentheses; $\epsilon_\infty = 78$.

typical of the central core of interwound DNA supercoils, the parallel cross-packed helical states observed in single-crystal X-ray data, and a low-energy extended square-planar intermediate. This low-energy form is different from the typical sugar–phosphate arrangement needed to construct the standard square-planar textbook models of a DNA four-way junction, e.g., Figure 1b. Here the conformations are consistent with the known bending preferences of adjacent base pairs into the major and minor grooves found in X-ray and solution studies, whereas the junctions of double-helical stems in the standard "open" model require large tilt angles of ~90° (stretching the sugar–phosphate backbone in one strand and compressing it in the complementary strand), which are not observed in low molecular weight nucleic acid analogs (Babcock & Olson, 1994). Our $\theta = 90°$ form, which like the others preserves the stacking and hydrogen-bonding interactions found in the B-DNA duplex (see below), is consistent with the maximum separation of duplex arms measured at low salt. While overall chain extension is greater if the arms of the junction are fixed at tetrahedral (109° 28′) angles, base stacking is also disrupted in such states. Preliminary attempts to build tetrahedral four-way junctions show that roll and tilt angles, as large as 70°, must be introduced at the crossover site (data not shown). As noted above, large tilting motions are not common even in unusual single-crystal nucleic acid structures [A. R. Srinivasan and W. K. Olson, unpublished observations from structures in the Nucleic Acid Database (Berman *et al.*, 1992)]. Disruption of DNA double helices is generally achieved by large rolling into the major and minor grooves or by twisting of adjacent base pairs (Zhurkin *et al.*, 1979, 1982). The set of optimized conformers reported here reveals a smooth pathway linking parallel and antiparallel spatial arrangements. According to a wide range of energy estimates, the interconversion does not present a significant barrier. The precise magnitude of the barrier, however, is still uncertain due to the approximate nature of the potential functions and the simplification of treating the DNA in the absence of explicit solvent and stabilizing counterions.

Notably, our predictions are supported by recent time-resolved fluorescence resonance energy transfer measurements (Eis & Millar, 1993) which reveal the occurrence in solution of an ensemble of conformational states of the four-way DNA junction. Moreover, the observed distributions of donor–acceptor distances suggest (1) that the DNA is divided into two domains corresponding to the extended helical arms in our models and (2) that the arms are subject to intramolecular motions over a range of states similar to the azimuthal variability seen in our computer models (Figure 5). In addition, our modeling is consistent with the gel mobilities of four-way helical junctions containing a nick at the point of strand exchange (Pöhler *et al.*, 1994). The stacked helical arms of the nicked structure appear to cross at an angle of 90°, adopting a state similar to our extended square-planar $\theta = 90°$ intermediate.

Conformational Interconversion. To move between one configuration and the next, the closely associated duplex arms of the Holliday structures simply rotate about the site of backbone strand exchange. At the base-pair level, the transition essentially involves a change in the roll angle between the residues abutting the exchange site. These conformational variations follow the known tendencies of double-helical DNA to bend preferentially along the roll rather than the tilt coordinate (Ulyanov & Zhurkin, 1984; Srinivasan *et al.*, 1987; Sarai *et al.*, 1989; Grzeskowiak *et al.*, 1993). Because the bases of the exchanged strands are located in different helical arms, there is neither unstacking nor disruption of Watson–Crick associations during the transition. The changes in roll angle are brought about simply by concerted variations of the torsion angles in the intervening (*i.e.*, crossover) chain backbones. The sugar–phosphate conformation, while generally different in the two single-stranded links in each junction, consistently directs the phosphate side-group oxygens away from the central pivot point of the junction. It is this stereochemical feature which ultimately facilitates the interconversion of one backbone arrangement to the next.

By contrast, the changes in base morphology and backbone geometry that must be introduced in the square-planar textbook and tetrahedral models are not "natural" conformational states of the double helix. The pathway to the open state from the compact (high salt) form does not follow the conventional conformational behavior of DNA and RNA (*i.e.*, a tendency to roll and twist rather than tilt adjacent base pairs). It has been suggested that the open four-way junction at low salt may resemble a transient intermediate in dynamic processes (such as isomerization and backbone manipulations) in branch migration (Clegg *et al.*, 1994). The conformational pathway needed to pass through an open unstacked square-planar or tetrahedral intermediate is not obvious. Aside from the "unnatural" conformational changes associated with the model, there is the additional problem of base-pair reasso-

ciation (*i.e.*, stacking) between open and closed forms to consider. The latter problem is avoided in the present model where base pairing and base stacking are preserved in all conformational states. Of course, the present scheme is highly approximate. Further refinement and improvement of the energy treatment will undoubtedly alter the idealized minimum energy structures presented here, although general conformational features (such as base stacking) are likely to persist.

The fact that the four-way junctions generated from arbitrary choices of helical packing exhibit rough morphological similarities with the unusual base-stacking geometries observed in a number of unrelated high-resolution nucleic acid single-crystal structures provides a measure of confidence in the computational approach. The modeling, in turn, points to potential new roles for the unusual backbone conformations observed experimentally. Similarities to known crystal structures are found for six of the eight sets of four-way junctions studied here. The local backbone torsions in the lowest energy models, however, are not necessarily related to those in the crystal structures. This is not surprising given the numerous ways that the sugar–phosphate chain backbone can generally link a given spatial arrangement of adjacent bases (Srinivasan & Olson, 1987).

The wide range of solutions associated with a given spatial arrangement of duplex arms provides some preliminary estimate of the entropic preferences for each configurational type. A conventional molecular dynamics simulation of junctions with arms at various azimuthal angles, of course, would provide a much more accurate estimate of the entropic contributions. Nevertheless, there are many more low-energy models built here with helices packed in an X than with axes that are perfectly parallel, antiparallel, or perpendicular to one another. The various electrostatic energy treatments, however, give different weight to crossed configurations ($\theta = \pm 45°$) that are more nearly parallel and those ($\theta = -135°$) that are closer to antiparallel. The different energy schemes may be mimicking the different environments encountered by a four-armed DNA junction in solution versus the closely packed array of helices found in the solid state.

While salt is treated approximately in this paper as condensed monovalent counterions, the general structural conclusions should remain unchanged if divalent ions are included in our scheme. Crossed configurations are observed experimentally only in the presence of Mg^{2+} ions and not under the simple ionic conditions of this study. It is unlikely that any of the conformers that we find would be ruled out or that new structures would be identified when Mg^{2+} is specifically treated. Note that the $\theta = 135°$ structure is disallowed by steric arguments and not by charge effects. Changes are likely, however, in the relative probabilities of different forms. It is well-known that cations have a profound effect on the structure of Holliday junctions. For example, the rate of branch migration is exceedingly sensitive to the type of cations present (Panyutin & Hsieh, 1994). It is beyond the scope of the current work, however, to study the stabilities of Holliday structures at different levels of counterion condensation and with different types of counterions.

Recombination Models. Analysis of the computer models of the four-way DNA junctions paves the way to understanding the detailed structural features involved in DNA recombination events. In several of the low-energy models the crossover site brings residues in the unexchanged strands into close contact, thereby facilitating further exchange. The secondary/induced crossovers can occur between the same strands involved in the initial junction or the two strands that do not participate in the first exchange. Additional linkages between the same strands will be formed only if the neighboring DNAs are aligned antiparallel ($\theta = \pm 180°$) or parallel ($\theta = 0°$) to one another. These two arrangements also bring residues in the unexchanged strands into close proximity. The latter contacts, separated from the first crossover site by 0.5, 1.5, 2.5, *etc.* helical turns, have recently been exploited in the three-dimensional molecular design of double crossover DNA molecules (Fu & Seeman, 1993). There are similar contacts between unexchanged strands when the helical arms of the Holliday model are crossed at angles of $-135°$ or $\pm 45°$. Only one of the many symmetrically related secondary contact points between unexchanged strands of perfectly antiparallel or parallel duplexes, however, persists in the crossed-strand arrangement. That is, the 45° variation in azimuthal angle relieves all close contacts between sites more than a half helical turn away from the branch point of the junction. The secondary contact points are displaced in the same sense (*i.e.*, in the 5′-direction) relative to the crossover point in the junctions with helical arms that are approximately parallel but in the opposite chemical sense (*i.e.*, one in the 3′-direction and the other in the 5′-direction) in the four-way structures that are antiparallel. These crossovers provide helpful clues for systematic future modeling of recombination structures, DNA knots, and other forms of multilinked DNA. The current models are closely related to the interactions between remote parts of longer DNAs. The crossed orientations of antiparallel duplexes found here are remarkably similar to the double-helical contacts found in long interwound supercoils (Hao & Olson, 1989; Zhang *et al.*, 1991; Yang *et al.*, 1993) and those introduced by the binding of DNA looping proteins (Zhang *et al.*, 1993). Moreover, the junctions with helical arms oriented at an angle of $-135°$ are consistent with the antiparallel interwound contacts formed by closed circular DNAs with a natural linking number deficit.

Branch Migration. Our morphological analysis of low-energy junctions confirms the commonly held notion that branch migration occurs more readily in parallel than antiparallel Holliday structures (Holliday, 1990). The crossover geometry most closely resembling the B-DNA duplex is the parallel (0°) model. The two states are related by a simple twisting and translational motion in the base-pair plane. All other branched structures, including the antiparallel form that predominates in solution, additionally involve a large roll angle between base pairs at the crossover site. Migration of the crossover site requires the exchange of the unusual backbone conformation at the crossover with the B-DNA geometry of the adjacent residues. This exchange of states and the consequent movement of the branch point will be far simpler if there is no need to flip (*i.e.*, roll) successive base pairs. Such major conformational rearrangements were not considered in recent models of branch migration derived from the trigonal packing in some crystals (Timsit & Moras, 1991). Except for the parallel configuration, it is necessary to disrupt base stacking and/or Watson–Crick pairing to transform the crossover linkages in the four-way junctions to standard B-form DNA (Olson *et al.*, 1983). Once the helical arms are aligned in a parallel state, however, the conformational change is accomplished with relatively little energetic cost by simultaneously over- and underwinding bases at the crossover sites. The necessary sliding motions can be achieved through correlated torsional changes about bonds, such as the P–O5′ in the $\theta = 0°$ four-way model (Figure 4), that are roughly parallel to the common vertical axis of the four-arm junction (Olson *et al.*, 1985). On a larger scale, these local changes

result in a slithering of closely packed helices past one another.

Comparison with Earlier Models. As emphasized above, there is no need to unstack bases during the interconversion of parallel and antiparallel branched configurations even though the overall shape of the four-way junction is radically altered during the process. The intermediate cross ($\theta = \pm 90°$) illustrated in Figure 5 with fully base stacked duplex arms is also noticeably different from the familiar square-planar textbook illustrations of the Holliday structure (*e.g.*, Figure 1b). The central void in the latter representation can be quite misleading in developing conformationally reasonable models. It is well-established that at high salt concentrations the DNA four-way junction folds into an X-form with pairwise stacking of helical arms (Cooper & Hagerman, 1989; Murchie *et al.*, 1989). NMR experiments show that base pairing and possibly base stacking is preserved at the site of branching over a wide range of temperatures (Wemmer *et al.*, 1985; Chen *et al.*, 1993). The molecular conformation under very low salt conditions, however, is not as well understood. There is general agreement that the junction adopts some sort of altered structure with extended helical arms (Cooper & Hagerman, 1989; Clegg *et al.*, 1994). However, there is some controversey as to whether such a structure is square-planar (as in standard textbook representations) or might include some pyramidal distorsions from planarity toward a tetrahedral form. Both forms necessitate an unusual tilting of base pairs that disrupts the stacking at the junction crossover and thereby creates a hole in the center of the four-way structure. These two models are consistent with the reactivity of osmium tetroxide with DNA four-way junctions at low salt (Paleček, 1992). The osmium-containing reagent is generally believed to react preferentially with single-stranded DNA, which might resemble the unstacked arrangements at the crossover sites in square-planar and tetrahedral junction models. It should be remembered, however, that osmium tetroxide also reacts with double-helical DNA containing subtle distinguishing features, such as alternating helical twist (McClellan *et al.*, 1986). Such conformational perturbations are present at the crossover sites of our extended junction with duplex arms oriented at $\theta = 90°$. Hence, it too may be consistent with the observed chemical reactivity studies of four-way junctions (McClellan *et al.*, 1986; Duckett *et al.*, 1988). A similar argument can be used to rationalize the altered chemical footprinting at 0 and 10 mM Mg^{2+} concentration of bimobile DNA junctions (in which two steps of branch migration are possible) (Lu *et al.*, 1990). The altered extended state of the junction might just as well be the 90°-stacked structure illustrated in Figure 5 as the open unstacked forms considered in the literature (Cooper & Hagerman, 1989; Murchie *et al.*, 1989).

Future Directions. The models reported here are only a starting point in the analysis of branched and supercoiled DNA structures. The generality of the methodology makes it possible to introduce double-helical arms of varying lengths, specific sequences (including long naturally curved DNA arms), relaxed base stacking at the crossover site, *etc.* The interactions between double-helical arms in the present series model may also serve as useful starting points in the analysis and design of binding ligands and proteins, such as histone H1 (Varga-Weisz *et al.*, 1993), specific to branched DNA molecules. It may be possible using the detailed representations of the nucleic acid backbone to develop compounds that lock different conformational arrangements of the Holliday structures.

ACKNOWLEDGMENT

Computations were performed at the Rutgers University Center for Computational Chemistry and through the facilities of the Nucleic Acid Database project (NSF Grant DIR 9012772). We thank Prof. Ned Seeman of New York University for helpful comments.

SUPPLEMENTARY MATERIAL AVAILABLE

An appendix describing computation of DNA groove widths, a table giving structural parameters of DNA double helices used to model four-way junctions, and a figure showing the distribution of phosphorus atoms in the central section of an idealized B-DNA duplex (4 pages). Ordering information is given on any current masthead page. Coordinates of four-way structures in Figure 5 are available from the authors.

REFERENCES

Babcock, M. S., & Olson, W. K. (1994) The effect of mathematics and coordinate system on comparability and "dependencies" of nucleic acid structure parameters, *J. Mol. Biol. 237*, 98–124.

Baikalov, I., Grzeskowiak, K., Tanagi, K., Quintana, J., & Dickerson, R. E. (1993) The crystal structure of the trigonal decamer C-G-A-T-C-G-^{6Me}A-T-C-G: A B-DNA helix with 10.6 base-pairs per turn, *J. Mol. Biol. 231*, 768–784.

Benjamin, H. W., & Cozzarelli, N. R. (1986) DNA-directed synapsis in recombination: Slithering and random collision of sites, *Proc. R. A. Welch Found. Conf. Chem. Res. 29*, 107–126.

Berman, H. M., Olson, W. K., Beveridge, D. L., Westbrook, J., Gelbin, A., Demeny, T., Hsieh, S.-H., Srinivasan, A. R., & Schneider, B. (1992) The nucleic acid database: A comprehensive relational database of three-dimensional structures of nucleic acids, *Biophys. J. 63*, 751–759.

Chandrasekaran, R., & Arnott, S. (1989) The structures of DNA and RNA helices in oriented fibers, in *Landolt-Börnstein Numerical Data and Functional Relationships in Science and Technology, Group VII/1b, Nucleic Acids* (Saenger, W., Ed.) Vol. 1, pp 31–170, Springer-Verlag, Berlin.

Chattopadhyaya, R., Ikuta, S., Grzeskowiak, K., & Dickerson, R. E. (1988) X-ray structure of a DNA hairpin molecule, *Nature (London) 334*, 175–179.

Chen, S.-M., Heffron, F., Leupin, W., & Chazin, W. J. (1991) Two-dimensional ^{1}H NMR studies of synthetic immobile Holliday junctions, *Biochemistry 30*, 766–771.

Chen, S.-M., Heffron, F., & Chazin, W. J. (1993) Two-dimensional ^{1}H NMR studies of 32-base-pair synthetic immobile Holliday junctions: complete assignments of the labile protons and identification of the base-pairing scheme, *Biochemistry 32*, 319–326.

Churchill, M. E. A., Tullius, T. D., Kallenbach, N. R., & Seeman, N. C. (1988) A Holliday recombination intermediate is twofold symmetric, *Proc. Natl. Acad. Sci. U.S.A. 85*, 4653–4656.

Clegg, R. M., Murchie, A. I. H., & Lilley, D. M. J. (1994) The solution structure of the four-way junction at low-salt conditions: A fluorescence resonance energy transfer analysis, *Biophys. J. 66*, 99–109.

Cooper, J. P., & Hagerman, P. J. (1987) Gel electrophoretic analysis of the geometry of a DNA four-way junction, *J. Mol. Biol. 198*, 711–719.

Cooper, J. P., & Hagerman, P. J. (1989) Geometry of a branched DNA structure in solution, *Proc. Natl. Acad. Sci. U.S.A. 86*, 7336–7340.

Cozzarelli, N. R., Boles, T. C., & White, J. H. (1990) Primer on the topology and geometry of DNA supercoiling, in *DNA Topology and its Biological Effects* (Cozzarelli, N. R., & Wang, J. C., Eds.) pp 139–184, Cold Spring Harbor Laboratory Press, Cold Spring Harbor, NY.

Duckett, D. R., Murchie, A. I. H., Diekmann, S., von Kitzing, E., Kemper, B., & Lilley, D. M. J. (1988) The structure of the Holliday junction, and its resolution, *Cell 55*, 79–89.

Duckett, D. R., Murchie, A. I. H., & Lilley, D. M. J. (1990) The role of metal ions in the conformation of the four-way junction, *EMBO J. 9*, 583–590.

Eis, P. S., & Millar, D. P. (1993) Conformational distributions of a four-way DNA junction revealed by time-resolved fluorescence resonance energy transfer, *Biochemistry 32*, 13852–13860.

Fenley, M. O., Manning, G. S., & Olson, W. K. (1990) Approach to the limit of counterion condensation, *Biopolymers 30*, 1191–1203.

Fenley, M. O., Olson, W. K., Tobias, I., & Manning, G. S. (1994) Electrostatic effects in short superhelical DNA, *Biophys. Chem. 50*, 255–271.

Fu, T.-J., & Seeman, N. C. (1993) DNA double-crossover molecules, *Biochemistry 32*, 3211–3220.

Grzeskowiak, K., Goodsell, D. S., Grzeskowiak, M. K., Cascio, D., & Dickerson, R. E. (1993) Crystallographic analysis of C-C-A-A-G-C-T-T-G-G and its implications for bending in B-DNA, *Biochemistry 32*, 8923–8931.

Hao, M.-H., & Olson, W. K. (1989) Searching the global equilibrium configurations of supercoiled DNA by simulated annealing, *Macromolecules 22*, 3292–3303.

Heinemann, U., Alings, C., & Bansal, M. (1992) Double helix conformation, groove dimensions, and ligand binding potential of a G/C stretch in B-DNA, *J. Mol. Biol. 210*, 369–381.

Hingerty, B. E., Ritchie, R. H., Ferrel, T. L., & Turner, J. E. (1985) Dielectric effects in biopolymers: The theory of ionic saturation revisited, *Biopolymers 24*, 427–439.

Hoess, R., Wierzbicki, A., & Abremski, K. (1987) Isolation and characterization of intermediates in site-specific recombination, *Proc. Natl. Acad. Sci. U.S.A. 84*, 6840–6844.

Holliday, R. (1964) A mechanism for gene conversion in fungi, *Genet. Res. 5*, 282–304.

Holliday, R. (1990) The history of the DNA heteroduplex, *BioEssays 12*, 133–142.

IUPAC–IUB Joint Commission on Biochemical Nomenclature (1983) Abbreviations and symbols for the description of conformations of polynucleotide chains, *Eur. J. Biochem. 131*, 9–15.

Jin, R., Chapman, W. H., Jr., Srinivasan, A. R., Olson, W. K., Breslow, R., & Breslauer, K. J. (1993) Comparative spectroscopic, calorimetric, and computational studies of nucleic acid complexes with 2′,5″ versus 3′,5″ phosphodiester linkages, *Proc. Natl. Acad. Sci. U.S.A. 90*, 10568–10572.

Joshua-Tor, L., Frolow, F., Appella, E., Hope, H., Rabinovich, D., & Sussman, J. L. (1992) Three-dimensional structures of bulge-containing DNA fragments, *J. Mol. Biol. 225*, 397–431.

Kitts, P. A., & Nash, H. A. (1987) Homology-dependent interactions in phage l site-specific recombination, *Nature (London) 329*, 346–348.

Kollman, P. A., Weiner, P. K., & Dearing, A. (1981) Studies of nucleotide conformations and interactions. The relative stabilities of double helical B-DNA sequence isomers, *Biopolymers 20*, 2583–2621.

Lavery, R. (1988) Junctions and bends in nucleic acids: A new theoretical modeling approach, in *DNA Bending and Curvature* (Olson, W. K., Sarma, M. H., Sarma, R. H., & Sundaralingam, M., Eds.) pp 191–211, Adenine Press, Schenectady, NY.

Lilley, D. M. J., & Clegg, R. M. (1993a) The structure of branched DNA species, *Q. Rev. Biophys. 26*, 131–175.

Lilley, D. M. J., & Clegg, R. M. (1993b) The structure of the four-way junction in DNA, *Annu. Rev. Biophys. Biomol. Struct. 22*, 299–328.

Lipanov, A., Kopka, M. L., Kaczor-Grzeskowiak, M., Quintana, J., & Dickerson, R. E. (1993) Structure of the B-DNA decamer C-C-A-A-C-I-T-T-G-G in two different space groups: Conformational flexibility of B-DNA, *Biochemistry 32*, 1373–1389.

Lu, M., Guo, Q., Mueller, J. E., Kemper, B., Studier, F. W., Seeman, N. C., & Kallenbach, N. R. (1990) Characterization of a bimobile DNA junction, *J. Biol. Chem. 265*, 16778–16785.

Lu, M., Guo, Q., Seeman, N. C., & Kallenbach, N. R. (1991) Parallel and antiparallel Holliday junctions differ in structure and stability, *J. Mol. Biol. 221*, 1419–1432.

Manning, G. S. (1978) The molecular theory of polyelectrolyte solutions with applications to the electrostatic properties of polynucleotides, *Q. Rev. Biophys. 11*, 179–246.

Mazur, J., & Jernigan, R. L. (1991) Distance-dependent dielectric constants and their application to double-helical DNA, *Biopolymers 31*, 1615–1629.

McClellan, J. A., Paleček, E., & Lilley, D. M. J. (1986) $(A\text{-}T)_n$ tracts embedded in random sequence DNA—formation of a structure which is chemically reactive and torsionally deformable, *Nucleic Acids Res. 14*, 9291–9309.

Miller, K. J. (1979) Interactions of molecules with nucleic acid structures with an application to the B-DNA structure and a counterclockwise helix, *Biopolymers 18*, 959–980.

Murchie, A. I. H., Clegg, R. M., von Kitzing, E., Duckett, D. R., Diekmann, S., & Lilley, D. M. J. (1989) Fluorescence energy transfer shows that the four-way DNA junction is a right-handed cross of antiparallel molecules, *Nature (London) 341*, 763–766.

Nauss, J. L. (1992) Conformational analysis of polynucleotides at the base-base level, Ph.D. Thesis, Rutgers University, New Brunswick, NJ.

Neidle, S., Taylor, G., Sanderson, M., Shieh, H.-S., & Berman, H. M. (1978) A 1:2 crystalline complex of ApA:proflavine: A model for binding to single-stranded regions in RNA, *Nucleic Acids Res. 5*, 4417–4422.

Nunes-Düby, S. E., Matsumoto, L., & Landy, A. (1987) Site-specific recombination intermediates trapped with suicide substrates, *Cell 50*, 779–788.

Olson, W. K., & Srinivasan, A. R. (1990) Classical energy calculations of DNA, RNA and their constituents, in *Landolt-Börnstein Numerical Data and Functional Relationships in Science and Technology, Group VII/1d, Nucleic Acids* (Saenger, W., Ed.) pp 415–435, Springer-Verlag, Berlin.

Olson, W. K., Srinivasan, A. R., Marky, N. L., & Balaji, V. N. (1983) Theoretical probes of DNA conformation. Examining the B → Z conformational transition, *Cold Spring Harbor Symp. Quant. Biol. 47*, 229–241.

Olson, W. K., Marky, N. L., Srinivasan, A. R., Do, K. D., & Cicariello, J. (1985) Theoretical studies of perturbed nucleic acid structures, in *Molecular Basis of Cancer* (Rein, R., Ed.) pp 109–121, Alan R. Liss, Inc., New York.

Olson, W. K., Srinivasan, A. R., Hao, M.-H., & Nauss, J. L. (1988) Base sequence dependent models of DNA curvature. The geometric interdependence of complementary residues, in *DNA Bending and Curvature* (Olson, W. K., Sarma, M. H., Sarma, R. H., & Sundaralingam, M., Eds.) pp 225–242, Adenine Press, Schenectady, NY.

Paleček, E. (1992) Probing DNA Structure with osmium tetroxide complexes *in vitro*, in *Methods in Enzymology* (Lilley, D. M. J., & Dahlberg, J. E., Eds.) pp 139–155, Academic Press, Inc., San Diego, CA.

Panyutin, I. G., & Hsieh, P. (1994) The kinetics of spontaneous DNA branch migration, *Proc. Natl. Acad. Sci. U.S.A. 91*, 2021–2025.

Pöhler, J. R. G., Duckett, D. R., & Lilley, D. M. J. (1994) Structure of four-way DNA junctions containing a nick in one strand, *J. Mol. Biol. 238*, 62–74.

Potter, H., & Dressler, D. (1976) On the mechanism of genetic recombination: Electron microscopic observation of recombination intermediates, *Proc. Natl. Acad. Sci. U.S.A. 73*, 3000–3004.

Potter, H., & Dressler, D. (1978) *In vitro* system from *Escherichia coli* that catalyzes generalized genetic recombination, *Proc. Natl. Acad. Sci. U.S.A. 75*, 3698–3702.

Ramstein, J., & Lavery, R. (1988) Energetic coupling between DNA bending and base pair opening, *Proc. Natl. Acad. Sci. U.S.A. 85*, 7231–7235.

Robertus, J. D., Ladner, J. E., Finch, J. T., Rhodes, D., Brown, R. S., Clark, B. F. C., & Klug, A. (1974) Structure of yeast phenylalanine tRNA at 3 Å resolution, *Nature (London) 250*, 546–551.

Robinson, B. H., & Seeman, N. C. (1987) Simulation of double-stranded branch point migration, *Biophys. J. 51*, 611–626.

Rubin, J., Brennan, T., & Sundaralingam, M. (1972) Crystal and molecular structure of a naturally occurring dinucleoside monophosphate. Uridylyl-(3′-5′)-adenosine hemihydrate. Conformational "rigidity" of the nucleotide unit and models for polynucleotide chain folding, *Biochemistry 11*, 3112–3128.

Sarai, A., Mazur, J., Nussinov, R., & Jernigan, R. L. (1989) Sequence dependence of DNA conformational flexibility, *Biochemistry 28*, 7842–7849.

Schlick, T., & Olson, W. K. (1992) Supercoiled DNA energetics and dynamics by computer simulation, *J. Mol. Biol. 223*, 1089–1119.

Schlick, T., Olson, W. K., Westcott, T., & Greenberg, J. P. (1994) On higher buckling transitions in supercoiled DNA, *Biopolymers 34*, 565–597.

Seeman, N. C. (1982) Nucleic acid junctions and lattices, *J. Theor. Biol. 99*, 237–247.

Seeman, N. C., & Kallenbach, N. R. (1983) Design of immobile nucleic acid junctions, *Biophys. J. 44*, 201–209.

Seeman, N. C., Sussman, J. L., Berman, H. M., & Kim, S. H. (1971) Nucleic acid conformation: Crystal structure of a naturally occurring dinucleoside phosphate (UpA), *Nature (London) 233*, 90–92.

Seeman, N. C., Maestre, M. F., Ma, R.-I., & Kallenbach, N. R. (1985) Physical characterization of a nucleic acid junction, in *The Molecular Basis of Cancer* (Rein, R., Ed.) pp 99–108, Alan Liss, New York.

Sigel, N., & Alberts, B. (1972) Genetic recombination: The nature of a crossed strand-exchange between two homologous DNA molecules, *J. Mol. Biol. 71*, 789–793.

Srinivasan, A. R., & Olson, W. K. (1980) Polynucleotide conformation in real solutions—A preliminary theoretical estimate, *Fed. Proc. 39*, 2199.

Srinivasan, A. R., & Olson, W. K. (1986) Conformational studies of (2′-5′) polynucleotides. Theoretical computations of energy, base stacking, helical structure, and duplex formation, *Nucleic Acids Res. 14*, 5461–5479.

Srinivasan, A. R., & Olson, W. K. (1987) Nucleic acid model building: The multiple backbone solutions associated with a given base morphology, *J. Biomol. Str. Dyn. 4*, 895–938.

Srinivasan, A. R., & Olson, W. K. (1992) DNA associations: Packing calculations in A-, B-, and Z-DNA structures, *Biophys. Chem. 43*, 279–310.

Srinivasan, A. R., Torres, R., Clark, W., & Olson, W. K. (1987) Base sequence effects in double helical DNA. I. Potential energy estimates of local base morphology, *J. Biomol. Str. Dyn. 5*, 459–496.

Takusagawa, F., Dabrow, M., Neidle, S., & Berman, H. (1982) The structure of a pseudo intercalated complex between actinomycin and the DNA binding sequence d(GpC), *Nature (London) 296*, 466–469.

Taylor, E. R., & Olson, W. K. (1983) Theoretical studies of nucleic acid interactions. I. Estimates of conformational mobility in intercalated chains, *Biopolymers 22*, 2667–2702.

Thompson, B. J., Camien, M. N., & Warner, R. C. (1976) Kinetic branch migration in double-stranded DNA, *Proc. Natl. Acad. Sci. U.S.A. 73*, 2299–2303.

Timsit, Y., & Moras, D. (1991) Groove-backbone interaction in B-DNA. Implication for DNA condensation and recombination, *J. Mol. Biol. 221*, 919–940.

Timsit, Y., Westhof, E., Fuchs, R. P. P., & Moras, D. (1989) Unusual helical packing in crystals of DNA bearing a mutation hot spot, *Nature (London) 341*, 459–462.

Timsit, Y., Vilbois, E., & Moras, D. (1991) Base-pairing shift in the major groove of $(CA)_n$ tracts by B-DNA crystal structures, *Nature (London) 354*, 167–170.

Ulyanov, N. B., & Zhurkin, V. B. (1984) Sequence-dependent anisotropic flexibility of B-DNA. A conformational study, *J. Biomol. Str. Dyn. 2*, 361–385.

Varga-Weisz, P., van Holde, K., & Zlatanova, J. (1993) Preferential binding of histone H1 to four-way helical junction DNA, *J. Biol. Chem. 268*, 20699–20700.

von Kitzing, E., Lilley, D. M. J., & Diekmann, S. (1990) The stereochemistry of a four-way DNA junction: A theoretical study, *Nucleic Acids Res. 18*, 2671–2683.

Wasserman, S. A., & Cozzarelli, N. R. (1986) Biochemical topology: Applications to DNA recombination and replication, *Science 232*, 951–960.

Wemmer, D. E., Wand, A. J., Seeman, N. C., & Kallenbach, N. R. (1985) NMR analysis of DNA junctions: Imino proton NMR studies of individual arms and intact junction, *Biochemistry 24*, 5745–5749.

White, J. H. (1989) An introduction to the geometry and topology of DNA structures, in *Mathematical Methods for DNA Sequences* (Waterman, M. S., Ed.) Chapter 9, CRC Press, Boca Raton, FL.

Yang, Y., Tobias, I., & Olson, W. K. (1993) Finite element analysis of DNA supercoiling, *J. Chem. Phys. 98*, 1673–1686.

Zhang, P., Olson, W. K., & Tobias, I. (1991) Accelerated record keeping Fourier series Monte Carlo simulations of an isotropic elastic rod model of DNA, *Comput. Polym. Sci. 1*, 3–17.

Zhang, P., Tobias, I., & Olson, W. K. (1994) Computer simulation of protein-induced structural changes in closed circular DNA, *J. Mol. Biol.* (in press).

Zhurkin, V. B., Lysov, Y. P., & Ivanov, V. (1979) Anisotropic flexibility of DNA and the nucleosomal structure, *Nucleic Acids Res. 6*, 1081–1096.

Zhurkin, V. B., Lysov, Y. P., Florentiev, V. L., & Ivanov, V. (1982) Torsional flexibility of B-DNA as revealed by conformational analysis, *Nucleic Acids Res. 10*, 1811–1830.